Research reports from Honors undergraduate students receiving support from the Shackouls Honors College via the Summer Research Fellowship

Summer 2018

Program Director:

Dr. Seth F. Oppenheimer

Edited by:

Katelyn Wright

MISSISSIPPI STATE UNIVERSITY™
JUDY AND BOBBY SHACKOULS
HONORS COLLEGE

Table of Contents

The Read Scare: Reading Stereotype Threat in College Aged Males

Rachel A. Booth

Psychology

Mississippi State University

Faculty Mentor, Department: Dr. Andrew F. Jarosz, Psychology

A common topic when discussing education is the gender gap in reading abilities. The Center on Educational Policy (Chudowsky & Chudowsky, 2010) found that in each grade and in each American state, girls outperformed boys on reading tasks. When children start primary school, teachers and parents assume that boys will require additional reading assistance compared to girls (Blair & Sanford, 2004). Furthermore, this disparity continues into secondary school. The Programme for International Assessment, an international survey given to 15 year olds, reported a reading gap between the genders that rates females 38 test points ahead of males – equivalent to a year's worth of progress (OECD, 2014). This gap persists even into upper education as English majors are nearly 75% women (Siebens & Ryan, 2009).

Research has suggested that this aptitude inequality could be caused by low self-concept (the belief that one can do a task well) in boys (Retelsdorf, Schwartz, & Asbrock, 2015), or by disinterest in the subject because reading is boring, difficult, and boys prefer TV (Sainsbury & Schagen, 2004). However, neither explanation attempts to address fundamental questions about the underlying reasons for boys' underperformance in reading. Rather than attributing boys' underperformance to innate gender differences in reading ability, as others have proposed, effects could be due to a stereotype threat (ST).

ST places people at risk of confirming a negative stereotype about a group with which they identify, leading to poorer task performance (Steele, 1997). Some work suggests that early differences in reading ability may indeed be due to stereotypes. For example, Pansu et al. (2016) demonstrated that third grade boys had poorer reading scores when they were placed under a negative reading stereotype than boys not under a stereotype. While there has been little consideration for stereotype threat in adult males, research dedicated to identifying the mechanisms underlying males' underperformance at reading is crucial, particularly when

considering the necessity of reading in daily life. The present study will therefore examine whether negative stereotypes exist for males on reading tasks, and whether these negative stereotypes affect reading ability.

Stereotype Threat

The ST phenomenon occurs when there is a societal perception of a group coinciding with an awareness of that belief from those included in the group (Aronson, Fried, & Good, 2002). In one of the few studies to consider a reading ST for boys, Pansu et al. (2016) demonstrated a reading ST effect for boys in their study. They assigned a reading test to 80 third graders, who were either told that the purpose of the study was to evaluate the children's reading ability, or to test out a new game. The gender by condition interaction revealed that the ST effect dramatically decreased boys' reading scores.

Though investigations of reading stereotypes in males are scarce, other common stereotypes have been studied, such as women underperforming in math (Spencer, Steele, & Quinn, 1998), or minorities having lower intelligence (Aronson, Quinn, & Spencer, 1998). In each of the aforementioned groups, subjects only underperformed when under the ST. The abundance and range of ST research lends confidence to the theory that ST interferes with task performance.

There are large numbers of women and minorities effected by ST, resulting in performances that are not congruent with their optimal capacity in areas such as mathematics for women and intelligence tasks for minorities (Aronson, Quinn, & Spencer, 1998; Nguyen & Ryan, 2008; Steele, 1997). In their lab, Steele and Aronson (1995) found that because of ST, African Americans' standardized test scores decreased. Another probable effect of ST is a lack of diversity in science, technology, engineering, and math fields (Shapiro & Williams, 2012).

Furthermore, those who suffer from ST have decreased ambition in jobs requiring the stereotyped ability (Davies, Spencer, Quinn, & Gerhardstein, 2002). They also tend to have low self-esteem (Aronson & Inzlicht, 2004) and even poor health (Blascovich, Spencer, Quinn, & Steele, 2001).

The most frequently studied targeted group is women, with research exploring how minute the ST has to be to alter performance results. Findings show ST can be induced easily – even being in a math class with a female math-confident teacher induces stress in female students who want to live up to their teacher's expectations (Shapiro, 2011). Likewise, simply having the individuals specify their own gender before a math task, having the experimenter note gender differences in the study, or the participant identifying with the task's subject matter can result in similar effects (Good & Aronson, 2008; Keller, 2007).

Working Memory Capacity

In well studied domains like mathematical performance in women, the existence and activation of ST has been established thoroughly enough, such that the mechanisms underlying ST have become a focus of research. In particular, studies have explored the role of working memory capacity (WMC). Beilock, Rydell, and McConnell (2007) demonstrated that WMC may be a primary mechanism underlying the effects of ST. Participants in both a control and ST condition were presented with math problems which demanded high or low WMC to solve. There was an interaction between ST and high demand problems, demonstrating that ST took a toll on WMC. Their results indicated that WMC resources are depleted by ruminations over the perceived stereotype and that depletion in WMC leads to a decrease in women's math solving abilities.

Counterintuitively, it may be high working memory participants who are most affected

by ST. Work examining choking under pressures suggests that high WMC subjects ordinarily use their capacity to employ more complex strategies and effective strategies on mathematical tasks (Beilock et al., 2007; DeCaro & Beilock 2010). Under high-pressure situations, however, some of this capacity is dedicated towards rumination, making these complex strategies more difficult to carry out. Higher WMC individuals are thus reduced to using low WMC strategies, removing their previous advantage. Low WMC individuals, who already tend towards simpler strategies, are less impacted. In other words, high pressure makes high WMC participants perform similarly to low WMC participants. If ST obeys similar mechanisms to choking under pressure, it may interact with WMC in the same way and strategy use will be rendered irrelevant under ST.

Because WMC is already known to be linked with reading ability, it is reasonable to expect similar ST effects on reading problems. Past research has found that scores on complex memory tasks, in both children and adults, predict reading achievement (Cain, Oakhill, & Bryant, 2004; Swanson, 2003; Swanson & Howell, 2001; Waters & Caplan 1996). Thus, WMC should predict reading scores under normal circumstances. However, under ST, the correlation between WMC and reading scores will not exist. In sum, WMC will be examined as a mediator through which the ST interferes with strategy use in high WMC males.

The Present Research

The gender reading gap is reminiscent of prior misconceptions of female underperformance on mathematical tasks. In that scenario, a body of literature has demonstrated that many gender differences in math ability are caused by negative stereotypes towards females (Good & Aronson, 2008; Keller, 2007; Nguyen & Ryan, 2008; Shaprio, 2011; Spencer, Steel & Quinn 1998).

The present study will determine if ST impacts reading task performance for college males. Male college students will complete a reading comprehension task, either with or without instructions intended to induce ST. They will additionally complete two WMC tasks. If ST is truly the cause of decreased reading scores among males, then high WMC men under ST will score lower on the reading task than high WMC men in the control group, with low WMC men unaffected by the manipulation. In contrast, women's reading scores will not be affected no matter the group.

Study 1.

Method

Design

The study will be a 2 (gender of participant) X 2 (ST or no ST) between-subjects factorial design.

Participants

A G*power analysis predicted that with 80 participants (40 in each condition) and 85% power assuming $\alpha = .05$, the study could detect an effect size of $d = .50$. Participants will be male and female college aged students.

Materials

The Gates-MacGintie Reading Test (GMRT). The GMRT (Gates & MacGintie 1993) is a commonly used reading comprehension task. It comes in two parts, reading comprehension and vocabulary; both will be used. In the first portion, participants will read 11 passages and then answer 3 to 5 questions for each passage. Gates-MacGinitie chose the passages from Arts and Science texts. The reading comprehension questions test both literal and inferential comprehension. Immediately following the reading comprehension, they will read 45 short

phrases with a word underlined and choose from five options which option best serves as a synonym for the underlined word. Form S, level AR will be used.

The Operation span. The automated Operation span (Ospan; Unsworth, Heitz, Schrock, &; Engle, 2005) is a commonly used test of WMC. The automated Ospan requires participants to solve a series of math problems interleaved with unrelated letters that they are expected to remember. Following the math/letter presentation, they are asked to recall the letters in the correct serial order. Sets range from three to seven letters in length, with three sets of each length. The computer scores participants' accuracy by summing all letters recalled in the correct serial order. All subjects will receive the exact same Ospan questions but in a randomized order.

The Symmetry span. The automated Symmetry span (Sspan; Unsworth, Redick, Heitz, Broadway, & Engle, 2009) is another common WMC test. In this computer automated task, subjects decide if varying shapes are vertically symmetrical. In between images of shapes to judge, red squares pop up on a random location in a grid and must be remembered. The red squares are recalled after participants judge several shapes and see several red squares, by clicking on the appropriate spaces in a grid in the correct serial order. Each of these lists include two to five squares, with three trials of each length. The Sspan consists of three trials.

The computer scores participants' accuracy by number of correct cells subjects clicked in correct order. Scores are calculated by summing the number of red square locations correctly recalled in the correct order.

Demographics Sheet. Following the tests, participants will receive a demographics sheet to collect gender, major, and age. Thirteen questions regarding academic reading exposure, reading identification, and awareness of the stereotype accompany the demographics.

Manipulation check. As part of the demographic information following the study, there will be a questionnaire including three items: "On a scale from 1-10, how much do you agree with this statement: 'The ability in reading comprehension of my gender is worse than the ability of the other gender.'"(Martiny, Roth, Steffens, & Croizet, 2012); "On a scale from 1-10, how much do you agree with this statement: 'I was motivated to perform well on the reading comprehension task to help show that I am good at reading."'(Yeung, von Hippel, 2008); and "On a scale from 1-10, how much do you agree with this statement: 'I was motivated to perform well on the reading comprehension task to help show that my gender is good at reading."'

The first rating will be reverse coded for females before being analyzed with the other two ratings. The mean of the ratings collected from these questions should indicate if participants believed the stereotype while completing the tasks.

Procedure

The study will be administered at Mississippi State University. Participants will be recruited through the SONA-systems website and will be given course credit as compensation.

Sessions will hold one to four subjects at a time. Instructions for both conditions will be presented by both the experimenter speaking to the participants, and by the participants reading the instructions on a sheet of paper while the experimenter speaks. Stereotype threat instructions for the reading task will be adapted from Beilock et al. (2007). Both groups will read and hear:

> "We are interested in reading comprehension. Most college subjects require advanced reading skills. However, not much is known regarding the mechanisms of reading abilities. This study is meant to discover what makes some people better at reading than others."

In the control condition, participants will also read and hear:

"Your performance on the reading problems you are doing today will be compared to other students in the nation."

In the experimental condition, subjects will also read and hear:

"As you may know, at most schools female students outnumber male students in majors requiring strong reading skills. There also seems to be a growing gap in academic performance between the two sexes. Unfortunately, there has not been a good explanation for this. Your performance on the reading problems you are doing today will be compared to female responses across the nation. Our specific research question is whether females are superior at all types of reading problems or only certain types."

Participants will first complete the GMRT. Then, each participant will complete both the Ospan and the Sspan, with the order of WMC task presentation counterbalanced. Participants who complete the WMC tasks before other participants will be given a filler task of completing a maze to do silently, while they wait for other participants to finish. The manipulation will be checked after the experiment is administered in a post-test questionnaire. After completing the post-test questionnaire, participants will be debriefed and the stereotype will be removed.

Results

A total of 120 participants completed all tasks in this study. A general linear model with gender and stereotype threat condition as fixed variables and working memory as a covariate demonstrated a main effect of gender, with male participants outperforming females on the Gates-MacGintie Reading Test, $F(1,42) = 6.168$, $p = .02$). However, there was no main effect of threat condition on performance, nor did any variables interact with gender. Rather, a significant working memory by threat condition interaction occurred, $F(1,42)= 6.552$, $p = .01$.

Discussion

This interaction demonstrated that when not under stereotype threat, working memory significantly predicted performance on the Gates-MacGintie Reading Test. However, when placed under a negative male stereotype, this relationship was eliminated. Surprisingly, neither men and women reacted to a negative male stereotype in this study. This suggests that reading ability is immune to stereotype threat due to expertise. To further examine this result, future studies will incorporate lengthier, harder texts. Additionally, science texts will be used to examine a interaction between males and reading, and women and science.

References

Aronson, J., Quinn, D. M., & Spencer, S. J. (1998). Stereotype threat and the academic underperformance of minorities and women. *Prejudice: The Target's Perspective*, 83-103.

Aronson, J., & Inzlicht, M. (2004). The ups and downs of attributional ambiguity: Stereotype vulnerability and the academic self-knowledge of African American college students. *Psychological science*, *15*(12), 829-836.

Aronson, J., Fried, C. B., & Good, C. (2002). Reducing the effects of stereotype threat on African American college students by shaping theories of intelligence. *Journal of Experimental Social Psychology*, *38*(2), 113-125.

Aronson, J., Lustina, M. J., Good, C., Keough, K., Steele, C. M., & Brown, J. (1999). When white men can't do math: Necessary and sufficient factors in stereotype threat. *Journal of Experimental Social Psychology*, *35*(1), 29-46.

Beilock, S. L., Rydell, R. J., & McConnell, A. R. (2007). Stereotype threat and working memory: mechanisms, alleviation, and spillover. *Journal of Experimental Psychology: General*, *136*(2), 256-276.

Blair, H. A., & Sanford, K. (2004). Morphing literacy: Boys reshaping their school-based literacy practices. *Language Arts*, *81*(6), 452-460.

Blascovich, J., Spencer, S. J., Quinn, D., & Steele, C. (2001). African Americans and high blood pressure: The role of stereotype threat. *Psychological science*, *12*(3), 225-229.

DeCaro, M. S., & Beilock, S. L. (2010). The benefits and perils of attentional control. In M. Csikszentmihalyi & B. Bruya (Eds.), *Effortless attention: A new perspective in the cognitive science of attention and action* (pp. 51–73). Cambridge, MA: MIT Press.

Gates, A. I., & MacGinitie, W. H. (1971). *Gates-MacGinitie reading tests*. Teachers College Press, Columbia University.

Cain, K., Oakhill, J., & Bryant, P. (2004). Children's reading comprehension ability: Concurrent prediction by working memory, verbal ability, and component skills. *Journal of educational psychology*, *96*(1), 31.

Davies, P. G., Spencer, S. J., Quinn, D. M., & Gerhardstein, R. (2002). Consuming images: How television commercials that elicit stereotype threat can restrain women academically and professionally. *Personality and Social Psychology Bulletin*, *28*(12), 1615-1628.

Gonzales, P. M., Blanton, H., & Williams, K. J. (2002). The effects of stereotype threat and double-minority status on the test performance of Latino women. *Personality and social psychology bulletin*, *28*(5), 659-670.

Hutchison, K. A., Smith, J. L., & Ferris, A. (2013). Goals can be threatened to extinction: Using the stroop task to clarify working memory depletion under stereotype threat. *Social Psychological and Personality Science*, *4*(1), 74-81.

Inzlicht, M., & Ben-Zeev, T. (2000). A threatening intellectual environment: Why females are susceptible to experiencing problem-solving deficits in the presence of males. *Psychological Science*, *11*(5), 365-371.

Keller, J. (2007). Stereotype threat in classroom settings: The interactive effect of domain identification, task difficulty and stereotype threat on female students' maths performance. *British journal of Educational Psychology*, *77*(2), 323-338.

Lefavrais, P. (1986). La pipe et le rat ou l'évaluation du savoir-lire du Cours Préparatoire à l'Enseignement Supérieur. *Paris: EAP*.

Levy, B. (1996). Improving memory in old age through implicit self-stereotyping. *Journal of Personality and Social Psychology*, *71*(6), 1092.

Logel, C., Walton, G. M., Spencer, S. J., Iserman, E. C., von Hippel, W., & Bell, A. E. (2009). Interacting with sexist men triggers social identity threat among female engineers. *Journal of personality and social psychology*, *96*(6), 1089-1103.

Martiny, S. E., Roth, J., Jelenec, P., Steffens, M. C., & Croizet, J. C. (2012). When a new group identity does harm on the spot: Stereotype threat in newly created groups. *European Journal of Social Psychology*, *42*(1), 65-71.

Nelson, M. J., Brown, J. I., & Denny, M. J. (1960). *The Nelson-Denny Reading Test: Vocabulary, Comprehension, Rate*. Houghton Mifflin.

Nguyen, H. H. D., & Ryan, A. M. (2008). Does stereotype threat affect test performance of minorities and women? A meta-analysis of experimental evidence.

OECD (2014). (Revised ed.). PISA 2012 Results: What Students Know and Can Do Student Performance in Mathematics, Reading and Science, Volume I,. PISA, OECD. (February 2014).

Pansu, P. Regner, I., Max, S., Colé, P., Nezlek, J.B., and Huguet, P. (2016) "A Burden for the Boys: Evidence of Stereotype Threat in Boys' Reading Performance." *Journal of Experimental Social Psychology* 65 (2016): 26-30.

Preacher, K. J., & Hayes, A. F. (2008). Asymptotic and resampling strategies for assessing and comparing indirect effects in multiple mediator models. *Behavior research methods*, *40*(3), 879-891.

Sainsbury, M., & Schagen, I. (2004). Attitudes to reading at ages nine and eleven. *Journal of Research in Reading*, *27*(4), 373-386. doi:10.1111/j.1467-9817.2004.00240.

Schmader, T., & Johns, M. (2003). Converging evidence that stereotype threat reduces working memory capacity. *Journal of personality and social psychology*, *85*(3), 440.

Shapiro, J. R. (2011). Different groups, different threats: A multi-threat approach to the experience of stereotype threats. *Personality and Social Psychology Bulletin*, *37*(4), 464-480.

Shapiro, J. R., & Neuberg, S. L. (2007). From stereotype threat to stereotype threats: Implications of a multi-threat framework for causes, moderators, mediators, consequences, and interventions. *Personality and Social Psychology Review*, *11*(2), 107-130.

Shapiro, J. R., & Williams, A. M. (2012). The role of stereotype threats in undermining girls' and women's performance and interest in STEM fields. *Sex Roles*, *66*(3-4), 175-183.

Shih, M., Pittinsky, T. L., & Ambady, N. (1999). Stereotype susceptibility: Identity salience and shifts in quantitative performance. *Psychological science*, *10*(1), 80-83.

Siebens, Julie, & Ryan, L., Camille (2012). Field of Bachelor's Degrees in the United States: 2009. *American Community Survey Reports.*

Steele, C. M. (1997). A threat in the air: How stereotypes shape intellectual identity and performance. *American Psychologist*, *52*(6), 613-629.

Steele, C. M., & Aronson, J. (1995). Stereotype threat and the intellectual test performance of African Americans. *Journal of Personality and Social Psychology*, *69*(5), 797-811.

Spencer, S. J., Steele, C. M., & Quinn, D. M. (1999). Stereotype threat and women's math performance. *Journal of Experimental Social Psychology*, *35*(1), 4-28.

Swanson, H. L. (2003). Age-related differences in learning disabled and skilled readers' working memory. *Journal of experimental child psychology*, *85*(1), 1-31.

Swanson, H. L., & Howell, M. (2001). Working memory, short-term memory, and speech rate as predictors of children's reading performance at different ages. *Journal of Educational Psychology*, *93*(4), 720.

Unsworth, N., Redick, T. S., Heitz, R. P., Broadway, J. M., & Engle, R. W. (2009). Complex working memory span tasks and higher-order cognition: A latent-variable analysis of the relationship between processing and storage. *Memory*, *17*(6), 635-654.

Yeung, N. C. J., & von Hippel, C. (2008). Stereotype threat increases the likelihood that female drivers in a simulator run over jaywalkers. *Accident Analysis & Prevention*, *40*(2), 667-674.

Name: Meghan Brino
Major: Biological Sciences
Faculty Mentor, Department: Dr. Janice E. Chambers, College of Veterinary Medicine, Center for Environmental Health Sciences

Title: Gene Expression Changes by Neuroprotectant Novel Antidotes to Organophosphates

ABSTRACT

Past assassinations and terrorist attacks demonstrate the need for a more effective antidote against nerve agents and other organophosphate (OP) compounds which cause brain damage through inhibition of the nervous system enzyme acetylcholinesterase (AChE). Our lab has designed novel phenoxyalkyl pyridinium oximes (U.S. patent 9,277,937) that demonstrate the ability to cross the blood-brain barrier and attenuate brain damage in a rat model. To evaluate these effects, this project determined whether rats treated with high levels of a surrogate for the nerve agent sarin (nitrophenyl isopropyl methylphosphonate; NIMP) and rats treated with NIMP followed by a novel oxime displayed significant differences in their levels of messenger RNA. RNA samples of brain regions susceptible to damage by seizure-inducing OP exposure levels (piriform cortex and hippocampus) from rats treated with NIMP alone or NIMP followed by a novel oxime were used in qPCR to examine expression levels of genes that reflect inflammation (CCL2) and nerve growth and repair (NGFR) in the piriform cortex, along with expression levels of genes involved in potential brain damage repair (BDNF) and astrocyte damage (GFAP) in the hippocampus. Changes in the levels of gene expression were compared across the experimental animal groups, i.e., NIMP alone, NIMP plus novel oxime, novel oxime alone, and vehicle controls. BDNF showed statistically significant transcriptional increases in several of the oxime and combination groups, indicating that novel oximes may be able to positively affect BDNF expression and thereby attenuate NIMP-related neuronal damage. Similarly, the novel oxime group stimulated the highest level of NGFR expression, again indicating novel oxime potential in brain cell repair. Though the other genes did not display statistical significance, average Ct values for NIMP, oxime, combination, and vehicle groups still demonstrated notable differences indicative of oxime therapeutic efficacy. Ultimately, these comparisons should demonstrate whether novel oximes can remediate some of the damage induced by NIMP poisoning and stimulate tissue repair. (Support: NIH U01NS083430.)

INTRODUCTION

Organophosphates (OP) consist of a diverse group of compounds with varied uses, including pesticides and nerve agents. OP inhibit acetylcholinesterase (AChE) in the central (CNS) and peripheral nervous systems (PNS). The subsequent buildup of acetylcholine in synapses leads to overstimulation of cholinergic receptors, potentially resulting in seizures, brain damage, or death. Two brain regions, the piriform cortex (PC) and hippocampus, exhibit damage following seizure-inducing levels of the nerve agent sarin (Spradling *et al.*, 2011).

The current treatment for OP poisoning involves atropine (a muscarinic receptor antagonist) and pralidoxime (2-PAM). 2-PAM is an oxime which reactivates inhibited AChE in the PNS but not the CNS, as it is unable to effectively cross the blood-brain barrier. Novel pyridinium oximes (U.S. patent 9,227,937; Figure 1) synthesized by this laboratory have provided convincing evidence of brain penetration and AChE reactivation *in vivo* using rats (Chambers *et al.,* 2013).

This lab uses non-volatile nerve agent surrogates which phosphorylate AChE with the same chemical moiety as their respective nerve agents, making them highly relevant for *in vitro* and *in vivo* use (Meek *et al.,* 2012). In this study, nitrophenyl isopropyl methylphosphonate (NIMP), a sarin surrogate, was employed (Figure 2).

Studies conducted by this lab have demonstrated altered gene expression in the rat piriform cortex following administration of high levels of NIMP. Some of the novel oximes were able to reverse these changes. The present research contributes data on the novel oximes' therapeutic capacity for attenuating brain damage by altering gene expression.

METHODS

Adult male (250-300g) Sprague Dawley-derived rats were administered SC either a high sublethal dosage of the sarin surrogate NIMP (0.325mg/kg) or vehicle (DMSO). At 1-hour post-NIMP exposure, peak inhibition (about 80%) of brain AChE and signs of hypercholinergic toxicity, including seizure-like behavior, occur. Rats were then administered IM 146 μmoles/kg of a novel oxime or 2-PAM in Multisol (48.5% H_2O, 40% propylene glycol, 10% ethanol, 1.5% benzyl alcohol) or the vehicle alone. The oxime dosage is equivalent to three human auto-injectors. Rats were euthanized 2 hours after oxime administration. The PC and hippocampus were quickly dissected, snap frozen, and stored at -80°C.

Following extraction, total RNA from both brain regions was purified using the RNeasy® Plus Mini Kit from Qiagen (Valencia, CA) and stored at -80°C. The purity and quantity of the samples were later determined using a Nanodrop ND-1000 spectrophotometer. The RT^2 First Strand Kit from Qiagen was used to reverse transcribe 0.5μg of total RNA into cDNA.

Duplex qPCR was performed on the Stratagene MX3005 qPCR system with IDT PrimeTime® qPCR Assays. The mRNA values were normalized using the housekeeping gene RPLP1. Each duplex qPCR was performed in triplicate in a final reaction volume of 20μl, using PrimeTime Gene Expression Master Mix and cDNA at empirically determined concentrations ranging from 36 to 75 ng. Three wells without template were included as negative controls. A total of 3 biological replicates and 9 technical replicates were collected for each treatment.

After normalization, mean Ct differences from each group were analyzed for outliers and normal distribution. Due to the lack of normal distribution, the Kruskal-Wallis test was used to test for statistically significant differences among the groups at $p < 0.05$. If a difference was found, the Mann-Whitney U test with a Bonferroni correction factor was used to determine which of the groups were statistically different at $p < 0.05$.

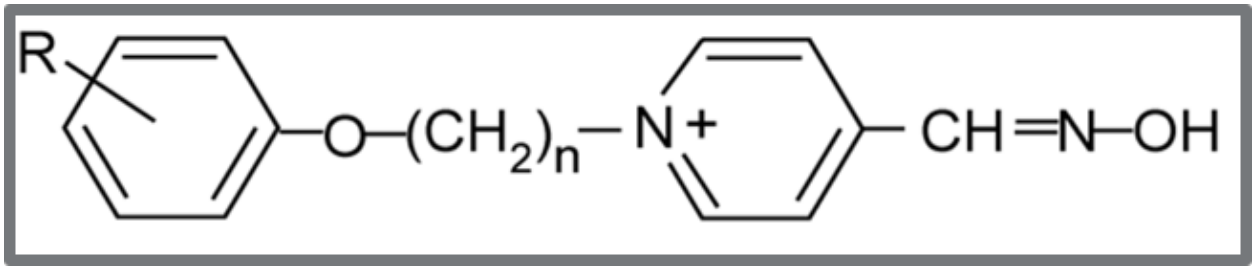

Oxime 1 n = 4 R = 4-Cl-

Oxime 20 n = 4 R = 4-Ph-CH_2–O-

FIGURE 1: Generic structure of novel substituted phenoxyalkyl pyridinium oximes, where **n** is the number of C's in the alkyl chain and **R** is the substitution on the phenoxy moiety.

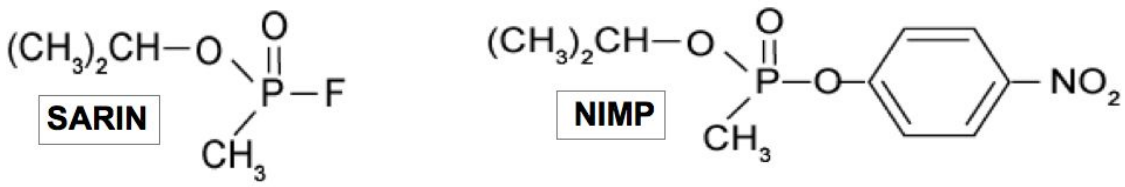

FIGURE 2: Structures of sarin and its surrogate, NIMP.

RESULTS

Hippocampal *BDNF* was the only gene to display statistically significant changes in expression (Table 1 and Figure 3). Expression was significantly increased when compared to the NIMP group for the 2-PAM, Oxime 20, and NIMP & 2-PAM groups.

	NIMP	2-PAM	Ox 1	Ox 20	NIMP & 2-PAM	NIMP & Ox 20	NIMP & Ox 1	Vehicles
NIMP		0.025	6.22	0.038	0.0011	1.17	0.067	2.32
2-PAM			0.016	2.32	5.95	0.15	1.45	0.19
Ox 1				0.055	0.0013	0.44	0.040	1.61
Ox 20					4.27	0.35	3.89	0.24
NIMP & 2-PAM						0.010	1.24	0.0087
NIMP & Ox 20							1.089	4.33
NIMP & Ox 1								0.27
Vehicles								

TABLE 1: Statistical differences in hippocampal *BDNF* expression across all experimental groups following treatment with either a high sublethal dosage of NIMP (0.325mg/kg) or vehicle (DMSO) followed 1 hour later with 146 μmoles/kg of a novel oxime or 2-PAM in Multisol or the vehicle alone (Multisol). P-values compare each individual group with the others. Significant values in red; values approaching significance in gray. Expression was significantly increased in comparison with the NIMP group for the 2-PAM, Oxime 20, and NIMP & 2-PAM groups.

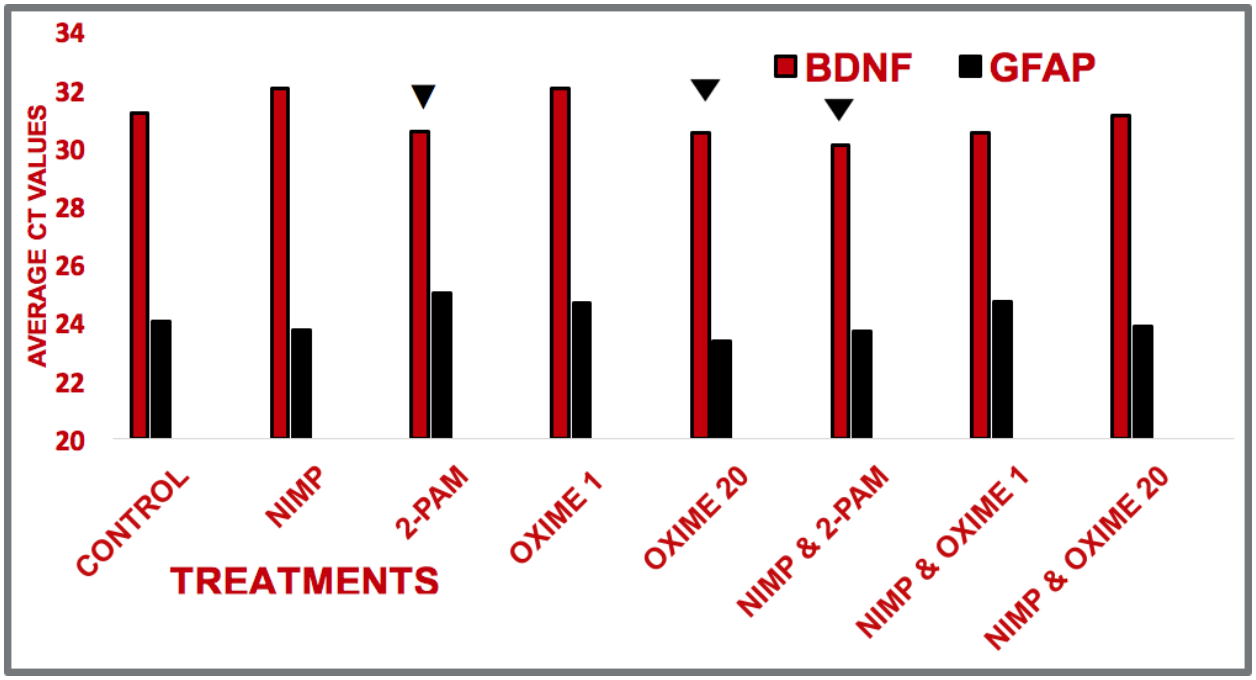

FIGURE 3: Hippocampal *BDNF* and *GFAP* average critical threshold (Ct) values following treatment with either a high sublethal dosage of NIMP (0.325mg/kg) or vehicle (DMSO) followed 1 hour later with 146 µmoles/kg of a novel oxime or 2-PAM in Multisol or the vehicle alone (Multisol). Lower values = greater expression. ▼ indicates a significant difference from the NIMP-only group at $p < 0.05$.

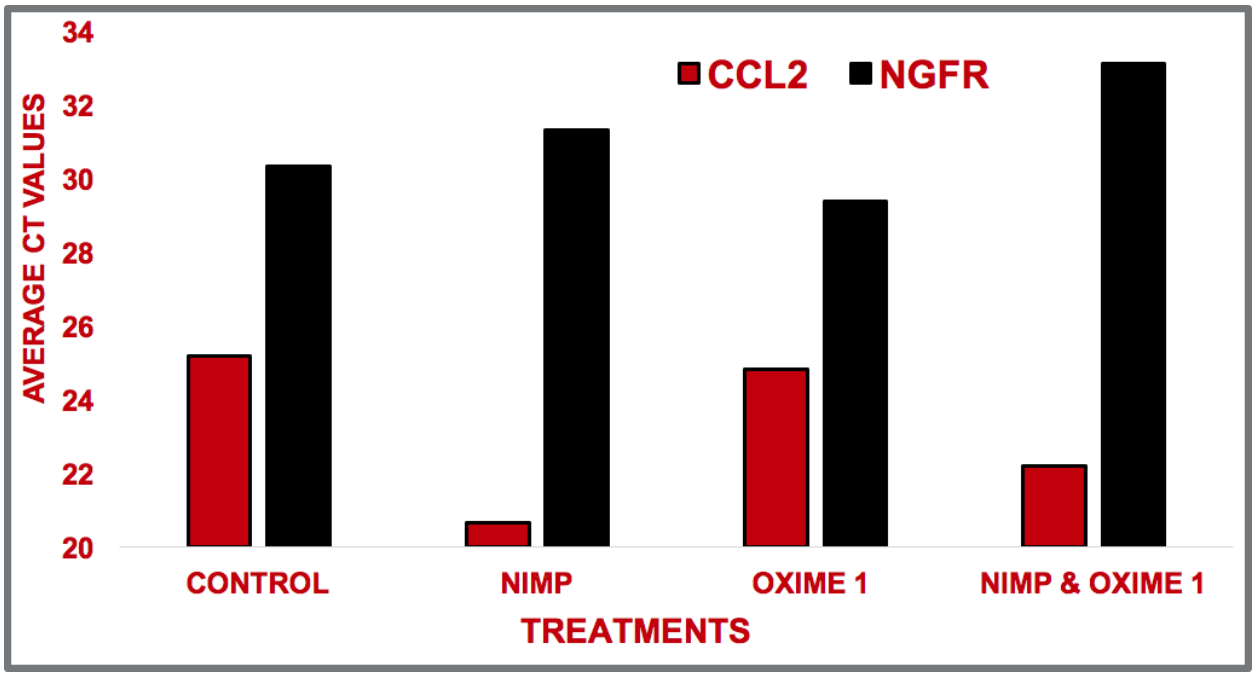

FIGURE 4: Piriform cortex *CCL2* and *NGFR* average critical threshold (Ct) values following treatment with either a high sublethal dosage of NIMP (0.325mg/kg) or vehicle (DMSO) followed 1 hour later with 146 µmoles/kg of Oxime 1 or 2-PAM in Multisol or the vehicle alone (Multisol). Lower values = greater expression.

DISCUSSION

BDNF

Compared to the NIMP-only group, BDNF expression was significantly increased by 2-PAM and Oxime 20 alone plus NIMP followed by 2-PAM. Although not statistically significant, NIMP alone and Oxime 1 alone both repressed BDNF expression to similar levels. However, NIMP followed by Oxime 1 or Oxime 20 reversed this effect by stimulating BDNF expression to a level equivalent to or greater than that seen for controls. As a neuroprotective gene, BDNF transcriptional increases prompt neuronal growth and repair (Lee *et al.,* 2016), so all three oximes were therapeutic after NIMP exposure.

GFAP

While not statistically significant, NIMP, Oxime 20, NIMP plus 2-PAM, and NIMP plus Oxime 20 all stimulated GFAP expression compared to control levels, whereas 2-PAM, Oxime 1, and NIMP plus Oxime 1 all repressed it. This suggests that Oxime 1, both alone and after NIMP exposure, may have therapeutic attributes since GFAP expression increases are associated with neural damage and neurodegeneration (Benkovic *et al.,* 2006).

CCL2

NIMP increased expression of CCL2, whereas both Oxime 1 alone and the NIMP plus Oxime 1 combination prompted decreased expression. Although the changes were not statistically significant, this decrease is therapeutic since CCL2 is a pro-inflammatory gene (Liu *et al.,* 2017).

NGFR

Oxime 1 increased expression compared to controls, but NIMP alone and the NIMP plus Oxime 1 combination decreased expression. This suggests that Oxime 1 is unable to overcome the effects of NIMP.

CONCLUSIONS

- Novel oximes increased expression of the neuroprotective gene *BDNF,* suggesting neuroprotection via brain cell growth and repair.
- Novel oximes decreased expression of the pro-inflammatory gene *CCL2,* indicating attenuation of the damage-inducing effects of inflammation.
- Novel oximes decreased expression of *GFAP*, which suggests a reduction of neural damage.

REFERENCES

Barrett GL, Naim T, Trieu J, Huang M. 2016. *In vivo* knockdown of basal forebrain p75 neurotrophin receptor stimulates choline acetyltransferase activity in the mature hippocampus. *J Neurosci Res* 94:389-400. doi: 10.1002/jnr.23717.

Benkovic SA, O'Callaghan JP and Miller DB. 2006. Regional neuropathology following kainic acid intoxication in adult and aged C57BL/6J mice. *Brain Res* 1070:215-231.

Chambers JE, Chambers HW, Meek EC, and Pringle RB. 2013. Testing of novel brain-penetrating oxime reactivators of acetylcholinesterase inhibited by nerve agent surrogates. *Chem Biol Interact* 203:135–138.

Lee WD, Wang KC, Tsai YF, Chou PC, Tsai LK, and Chien CL. 2016. Subarachnoid hemorrhage promotes proliferation, differentiation, and migration of neural stem cells via *BDNF* upregulation. *PLoS One* Nov 10;11(11):e0165460. Doi: 10.1371/journal.pone.0165460.

Liu H, Davis JRJ, Wu Z and Abdelgawad AF. 2017. Dexmedetomidine attenuates lipopolysaccharide induced *MCP-1* expression in primary astrocyte. *Biomed Res Int* Volume 2017, Article ID 6352159, 6 pages, doi:10.1155/2017/6352159.

Meek EC, Chambers HW, Coban A, Funck KE, Pringle RB, Ross MK and Chambers JE. 2012. Synthesis and *in vitro* and *in vivo* inhibition potencies of highly relevant nerve agent surrogates. *Toxicol Sci* 126:525-533.

Spradling KD, Lumley LA, Robison CL, Meyerhoff JL, and Dillman JF. 2011. Transcriptional responses of the nerve agent-sensitive brain regions amygdala, hippocampus, piriform cortex, septum, and thalamus following exposure to the organophosphonate anticholinesterase sarin. *J Neuroinflammation* 8:84. doi: 10.1186/1742-2094-8-84.

Name: Mayukh Datta

Major: Chemical Engineering

Faculty Mentor and Graduate Student: Dr. Neeraj Rai and Zachary Windom

Understanding Condensed Phase Structure and Dynamics of Herbicides using First Principle Molecular Dynamics Simulations

Introduction

Nonpoint source pollution from herbicides is a significant environmental issue, disproportionately affecting rural and underprivileged communities in the United States. Glyphosate, a common herbicide that readily binds to soil constituents yet is easily soluble in water, has come under a lot of scientific scrutiny and is thought to be carcinogenic. Glyphosate (*N*-phosphonomethyl glycine), a common herbicide that readily binds to soil constituents yet is easily soluble in water, has come under a lot of scientific scrutiny and is thought to be carcinogenic. Therefore, to design efficient separation processes and to aid epidemiological studies of the effect of glyphosate on humans, the conformational flexibility and structural characteristics of glyphosate in aqueous solution must be understood.

Methodology

This work utilizes ab initio molecular dynamics (AIMD) simulations to study the behavior of the glyphosate molecule in aqueous phase under equilibrium conditions. Previous metadynamics simulations were conducted by my mentor, Zachary Windom, and suggested that beyond a certain torsion angle, the carboxylic group in the glyphosate molecule is completely deprotonated. To determine the structural stability of glyphosate at equilibrium conditions, I ran normal NVT simulations using CP2K to determine the dihedral profile of glyphosate, and in doing so, I strengthened my programming knowledge and learned how to create input files for

CP2K calculations. Lastly, I learned and utilized TRAVIS to generate plots of radial distribution function, hydrogen bond analysis, and infra-red spectra.

Results: As shown by the radial distribution function on Figure 1c, there appears to be a presence of a hydrogen bond between H6 and O, with the first solvation shell peaking around 1.5 A and ending around 2.5 A. This is further affirmed by Figure 2 where in the hydrogen bond autocorrelation function of H6-O had one of the largest lifespans. Lastly, as shown in Figure 3, we concluded that the peak around 1600 corresponds to the carboxylic acid group and the triple peaks at 3200 cm^{-1}, 3400 cm^{-1}, and 3600 cm^{-1} corresponds to CH_2, NH_2, and POOH groups.

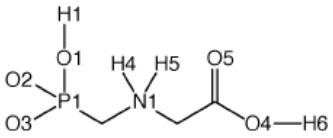

Glyphosate Molecule

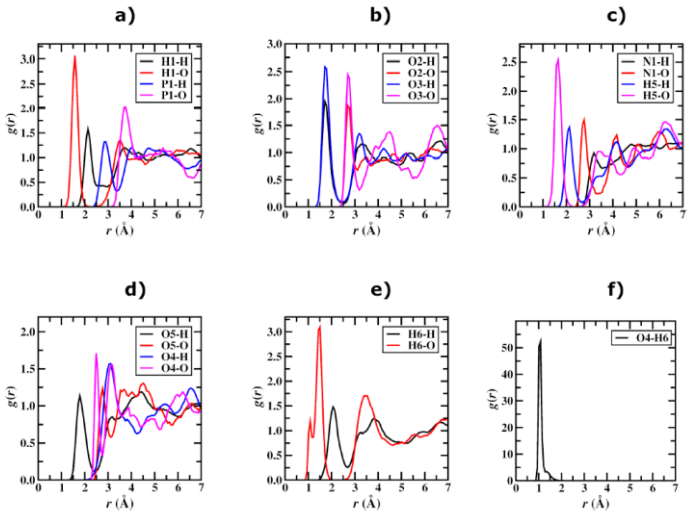

Figure 1: Radial Distribution Function

Shows the probability of encountering a hydrogen or oxygen atom within a water molecule. The numbered atoms represent atoms on the glyphosate molecule while the non-numbered atoms represent those in the water molecule.

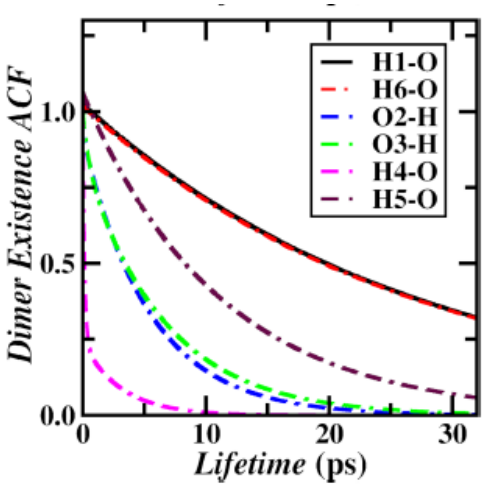

Figure 2: Hydrogen Bond Autocorrelation Function

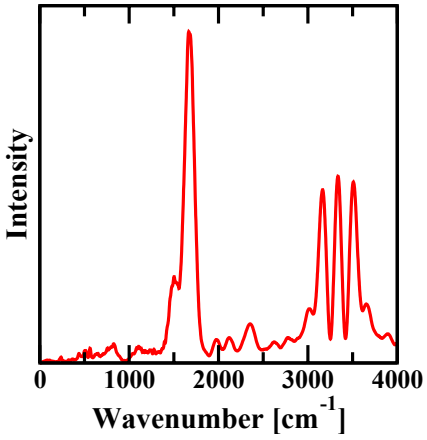

Figure 3: Infrared Spectra

Conclusion:

Through metadynamics simulations of intramolecular proton transfer reactions conducted by Zachary Windom, it was established that glyphosate predominately existed in its zwitter ion form. Furthermore, as concluded by the radial distribution function, we realized that glyphosate was persistent in aqueous conditions and had significant hydrogen bonding at H6 location on the carboxylic group. Furthermore, moderately strong hydrogen bonding occurred at the H5 location on the amine group and the O2 location on the phosphonate group. Knowledge about the presence of these hydrogen bonds could aid future biomedical and separations research wherein most simulations do not allow for bond breaking.

Reference:

C. N. Albers, G. T. Banta, P. E. Hansen, and O. S. Jacobsen, "The influence of organic matter on sorption and fate of glyphosate in soil–Comparing different soils and humic substances," Environmental pollution, vol. 157, no. 10, 2009, pp. 2865–2870.

W. Battaglin, M. Meyer, K. Kuivila, and J. Dietze, "Glyphosate and its degradation product AMPA occur frequently and widely in US soils, surface water, groundwater, and precipitation," JAWRA Journal of the American Water Resources Association, vol. 50, no. 2, 2014, pp. 275–290.

S. O. Duke and S. B. Powles, "Glyphosate: a once-in-a-century herbicide," Pestmanagement science, vol. 64, no. 4, 2008, pp. 319–325.

Name: Gwyneth Jones
Major: Wildlife, Fisheries, and Aquaculture

Faculty Member, Department: Dr. Marcus Lashley, Wildlife, Fisheries, and Aquaculture

Title: *Monitoring Vulture Response to Temporally Varied Carrion Supplement*

Introduction:

Vultures provide several ecosystem services including vertebrate remains disposal, nutrient redistribution, and carcass decontamination (Ogada et al 2012, Mateo-Tomas et al 2017). Because vultures are the only obligate vertebrate scavengers, they are particularly efficient in locating and consuming carrion. As such, without vulture provision of these ecosystem services, the associated processes may be disrupted. New and old-world vultures are declining worldwide (IUCN Redlist 2018). Causes of this decline vary, but the majority of vultures face decline due to persecution, poisoning (inadvertent or deliberate), and decline in food supply related to overhunting, with vultures experiencing the most rapid declines affected by all three causes (Ogada and Keesing 2012). Supplemental feeding is a common method used for supporting declining vulture populations, but the effectiveness of this conservation technique has not been evaluated (Cortes-Avizanda et al 2016). Additionally, it has been noted that "vulture restaurants," or sites of repeated carrion application on the landscape, may result in dominance interactions between vulture species that influence resource utilization (Cortez-Avizanda 2012).

Mass mortality events (MMEs) are population mortality events that take place in a restricted time and space (Baruzzi et al. 2018). They can be triggered by several causes among which are disease outbreaks or environmental changes. MMEs causes are exacerbated due to climate change so that these events are increasing in magnitude and occurrence (Fey at al. 2015). MMEs have the potential for greater ecological impact than typical sources of carrion due to greater quantities of biomass (Baruzzi et al. 2018). In fact, several species, among which are vultures, can be attracted by the carrion pulse generated by a MME. Vultures would be beneficial for recycling carrion from MMEs, and MMEs can be an important resource for vultures. We wanted to investigate vulture response to MMEs by evaluating the response of common North American vulture species, black vultures (*Coragyps atratus*) and turkey vultures (*Cathartes aura*), to various methods of supplemental feeding. Using large recurrent carrion amounts, we also wanted to determine the best practices for supplementing vultures while minimizing intraspecific competition.

Methods:

2017 and 2018 carrion deployment experiments were performed in Panther Swamp National Wildlife Refuge, with carrion provided by the cullings of feral swine (*Sus scrofa*) by the USFWS as a method of population control.

Supplemental feeding experiments in the summer and fall of 2017 observed the response of scavengers to carrion application from August to November. The experiment was carried out in three sites, each containing four plots (10 m diameter), at least 250 meters apart from each

other. In each plot, one horizontal camera and one vertical camera was deployed. The horizontal cameras were secured so that they collected data parallel to the ground. The vertical cameras were affixed to the top of tripods, centered over a carcass, and pointed towards the ground to collect top-down data. Three months of deployment were chosen: August, September, and October. One plot, which was subjected to the first treatment in each site, had approximately 300 pounds of carrion applied each month of deployment. The other three plots each had carrion deployed in only one of the three months. This design allowed for the examination of the effects of carrion supplementation in different seasons, particularly around the time period where North American vultures prepare for and begin migration. It also allowed for the observation of the effects of vulture restaurants.

Supplemental feeding experiments in the summer of 2018 were designed to observe the effects of short-term temporal variations in carrion application. Three sites, each containing two plots within old growth forest, were selected for the experiment. Plots were randomly selected circular areas of 78.5 m^2 (10 m diameter) that were at minimum 250-400 meters apart. One plot in each site had its entire lot of carrion, approximately 470 pounds, applied at one time in early July. The second plot in each site had the same quantity of carrion as the first plot applied over three deployments, each ten days apart, beginning on the same deployment date as the first plot's deployment. At each plot, two camera traps were set up to collect data. One camera trap collected horizontal data, while the other camera was affixed to a large tripod over the deployed carrion to collect vertical (top-down) data.

Data was collected from both types of cameras after the conclusion of these experiments and analyzed for species richness, quantities, and activity in various treatments.

Additional Methods on Additional Data for Side Project:

Vertical cameras in both experiments served to allow for detection of species that may not be observed from horizontal camera data. It was designed to improve species identification in landcover types that may inhibit the detection of some scavenger species. Comparisons of vertical and horizontal camera trap detection of species we performed on the 2017 data found that the addition of vertical camera traps aided in identification of species in adverse landcover types (O'Connell et al 2018). As other scavengers may influence vulture behavior, accurate detection of these species is key to understanding the response of target species to carrion supplementation

Progress:

In the summer and fall of 2018, horizontal camera data from the carrion deployment experiments of 2018 were analyzed for species counts, behaviors, and activity while the experiments of Summer 2018 were carried out. Preliminary analyzes run on the 2017 data detected no difference in the overlaps in black vulture activity with turkey vulture activity across treatments. The lack of difference in activity might be due to the limited nature of the study. Three carrion deployments may be inadequate to induce the change observed in studies with other species (Cortes-Avizanda 2012). However, a sharp drop in vulture activity between the months of August-October and November was detected. Possible explanations include

reduction in local vulture populations due to seasonal migrations and response of vulture to hunting. While several hunting seasons open in October, the majority open beginning in November and continuing into the winter months. Vultures may seek out the remains of harvested animals left by hunters, resulting in lower vulture numbers at experimental plots. Data from the summer of 2018 was retrieved at the conclusion of the summer experiments.

Future Work:

In the coming months, analysis of the summer 2018 data for species richness, quantities, and activity in various treatments will be performed. After this is completed, the data will be evaluated to determine whether temporal variation and repeated application influence vulture colonization. This will allow for the development of management practices that may improve vulture utilization of supplemental carrion, while reducing the use of applied carrion by non-target scavengers. By favoring vulture utilization of carrion over non-vulture vertebrate scavengers, the spread of disease from carrion may be reduced, particularly if resulting from MMEs. Further analysis on 2017 data will involve observation of interspecies scavenger interactions, including trends in activity of non-vulture vertebrate scavengers. The research performed in the summer of 2018 will be presented at Mississippi State University's Spring Undergraduate Research Symposium.

~~Works Cited~~References:

Baruzzi, C., Mason, D., Barton, B., & Lashley, M. (2018). Effects of increasing carrion biomass on food webs. *Food Webs*, *17*, e00096.

Cortes-Avizanda, A., Blanco, G., DeVault, T.L., Markandya, A., Virani, M.Z., Brandt, J., and J.A. Donazar. (2016). Supplementary feeding and endangered avian scavengers: benefits, caveats, and controversies. Frontier in Ecology and the Environment, 14(4):191-199.

Cortes-Avizanda, A., Jovani, R., Carrete, M., and J.A. Donazar. (2012). Resource unpredictability promotes species diversity and coexistence in an avian scavenger guild: a field experiment. Ecological Society of America, 93(12):2570-2579.

Fey, S. B., Siepielski, A. M., Nusslé, S., Cervantes-Yoshida, K., Hwan, J. L., Huber, E. R., ... & Carlson, S. M. (2015). Recent shifts in the occurrence, cause, and magnitude of animal mass mortality events. *Proceedings of the National Academy of Sciences*, *112*(4), 1083-1088.

IUCN Redlist. (2018). The IUCN Red List of Threatened Species. www.iucnredlist.org Accessed March 16, 2018.

Mateo-Tomas, P., Olea, P.P., Moleon, M., Selva, N., and J.A. Sanchez-Zapata. (2017). Both rare and common species support ecosystem services in scavenger communities. Global Ecology and Biogeography, 26:1459-1470.

O'Connell, C., Baruzzi, C., Mason, D., Jones, G., Cove, M., Barton, B., and M. Lashley. (2018). Horizontal and Vertical Camera Trapping Designs Produce Different Species Richness in Carrion Food Webs. The Wildlife Society National Conference.

Ogada, D.L., Keesing, F., and M.Z. Virani. (2012). Dropping dead: causes and consequences of vulture population declines worldwide. New York Academy of Sciences, 1249:57-71.

Ogada, D.L., Torchin, M.E., Kinnaird, M.F., and V.O. Ezenwa. (2012). Effects of vulture declines on facultative scavengers and potential implications for mammalian disease transmission. Conservation Biology, 26(3):453-460.

Name: Maleen Wijeratna Kidiwela

Major: Professional Geology

Faculty Mentor, Department: Dr. Varun Paul, Geosciences

Title: Influence of Geomagnetic Fluctuations on Temporal Atmospheric Water Vapor Variability

Introduction

The geomagnetic field, which is responsible for shielding Earth from incoming cosmic radiation, is currently 10 percent weaker than it was in 1845. Growing concern about the effect of this weakening on Earth processes has resulted in several recent studies focused on quantification of geomagnetic variability via satellites and ground stations. Although the extent and sophistication of geomagnetic observations have grown rapidly in recent years, the potential influence of geomagnetic variability on environmental and climatological processes remains largely unexplored. This study focuses on identifying and understanding a potential relationship between geomagnetic fluctuations and temporal water vapor variability using an experimental approach.

Methods

Mechanisms of experimental approach was based upon a complete construction/ design of a molecular behavior tracking tank. The tank designs enable observing the behavior of atomized water through digitalized data. The design principle keeps track of the behavior of particles through recording the intensity of twelve, 680nm laser passing through a glass tank. Any disturbances to each individual laser beam by the water molecules lying in its path would register as a decline in the intensity of the laser. The laser intensity is measured through a series of 12 individual photodiodes that generates a current based upon the intensity of light. Each photodiode lies in the other end of the laser beam located at the opposite side of the tank. Figure 1 indicates the four separate vertically oriented planes (indicated as 1,2,3,4) partitioned to 3 horizontal planes (indicated as top, mid, bot) stacked on top of each other. Each line of intersection between the vertical and the horizontal planes traces laser pathways running through the tank. The tank dimensions are 12” x 12” x 12”. The 3L reservoir of water made within the tank was used to atomize the water and fill up the unoccupied volume of the tank with water vapor. The ultrasonic atomizer releases fine water particle in to the air through subjecting water to ultrasonic vibrations through a piezo-electric plate. Fine particles of water produced for this experiment is used to simulate the behavior of atmospheric water reservoir located in higher altitudes. The particle size of the water droplets generated by ultrasonic atomization are mostly within 70 to 80 μm range (Dalmoro et.al). The droplets produced with less than 100 μm are easily manipulatable by varying methods of induced force.

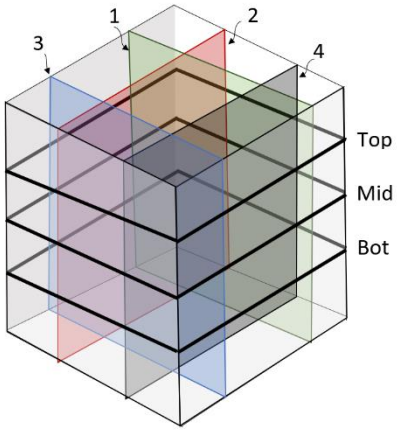

Fig.1

A total of 5 types of experiments were performed with each repeating for at least 10 times. Repeated experiments were used to remove discrepancies lying within the data such as background noise. In order to minimize the background influence of electromagnetic waves in the surrounding environment, the whole setup was covered by a faraday foil cage. Faraday cage preparation material from ‘Faraday Defense’

provides 45db electromagnetic interference (EMI) attenuation, 10nJ electro-static discharge (ESD) shielding through foil thickness of 7.0mil (0.14mm). Furthermore, to stabilize the readings obtained through the photo-diodes, the experiments were carried out within a dark room. In order to avoid adhesion of water molecules to the tank surface, a hydrophobic material with anti- fog properties was coated before each experiment.

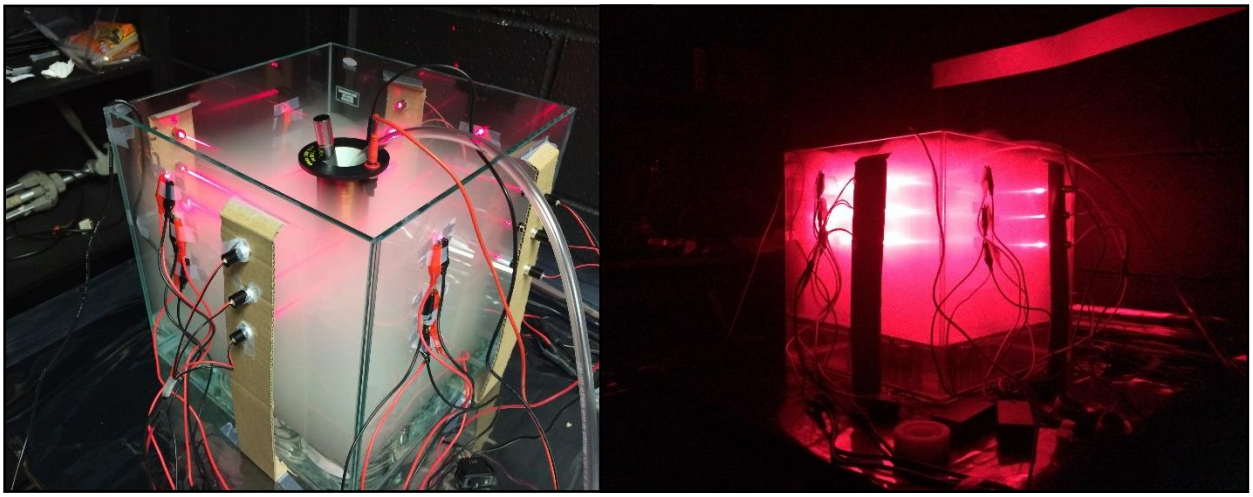

Fig.2: Magnetic Cloud Chamber

Water vapor dissipation experiment with a constant magnetic field (97 μt) and a varying magnetic field (1Hz, 97 μt).Temporal changes in behavior of particles were measured before and after subjecting to a constant magnetic field using 10 experiments that were carried out by changing the magnetic input within 20 Minutes. During the experiment, first 1-5 Minutes measured with no Magnetic Field, 5-10 Minutes with Constant Magnetic Field (97 μT), from 10-15 Minutes with no magnetic field, and from 15-20 Minutes with Varying Magnetic Field (1 Hz, 97 μT). Changes in frequency of magnetic variation with behavior of water particles was experimented using, 5 experiments were conducted with changing the magnetic fluctuations. First 1-5 Minutes with no Magnetic Field, from 5-10 Minutes with 0.0005 khz Fluctuation in 97 μt, from 10-15 Minutes with 0.001 khz Fluctuation 97 μT, from 15-20 Minutes with 0.01 khz Fluctuation 97 μT, from 20-25 Minutes with 1 khz fluctuation 97 μT, and from 25-30 minutes with no magnetic field. Changes in magnitude of magnetism with behavior of water particles were measured using 5 experiment each having the following separate variations. First 1-5 minutes with no magnetic field, starting 5 minutes to 10 minutes with 58 μT, from 10-15 minutes with 97 μT, from 15-20 minutes with 141 μT and from 20-25 Minutes retested with no magnetic Field

Results

The data obtained by the five separate experiments were used to support the hypothesis. The water vapor dissipation experiment was conducted with a constant and varying magnetic fields. The Figure 3 represents the stacked averages of 10 separate experiments for each type of dissipation experiment. According to the Figure, the average total time taken to dissipate the full volume of atomized water vapor without the magnetic field was observed to be 230 Seconds. The induced constant magnetic field reduced the dissipation time to 190 seconds. The Lowest average dissipation time of 170 seconds was recorded when a fluctuating magnetic field (1 Hz) was induced.

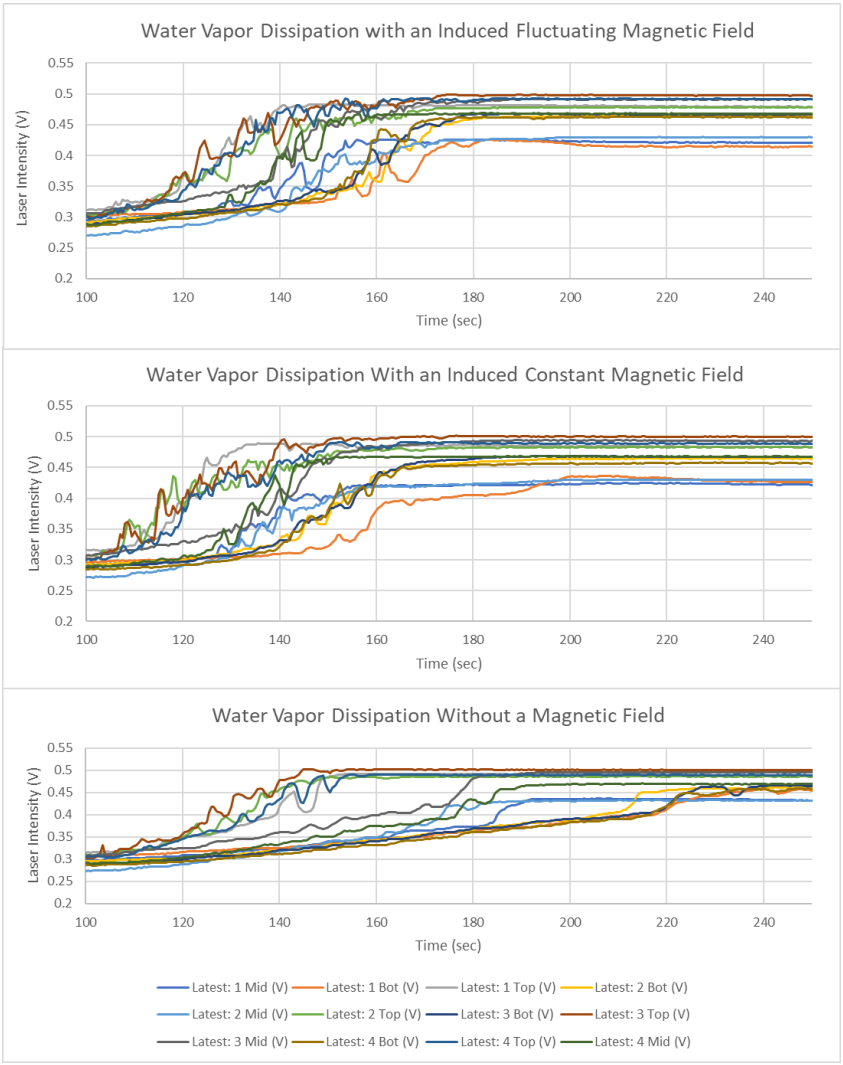

Fig.3

The Figure 4 shows the variations of the laser intensity observed in each photodiode (Standard deviation within each time interval). When the magnetic field was turned on (Both Varying and constant magnetic field), the values observed in each sensor had changed drastically. The variations of the laser intensity recorded during the time periods of no magnetic field, exhibited similar trends although the two 'no magnetic field' readings were obtained on two separate times very well isolated within the experiment.

The Figure 4 shows the average intensity recorded on all sensors response to varying magnetic field fluctuations. Thus, the intensity of all 5 magnetic fluctuation experiments peaked at 0.01 KHz. This indicates that the water vapor content in each laser array had a significant reduction with the increase of the frequency of fluctuation until a threshold frequency was reached. A separate experiment was carried out to determine the influence of the magnitude on the water vapor measured in terms of laser intensity.

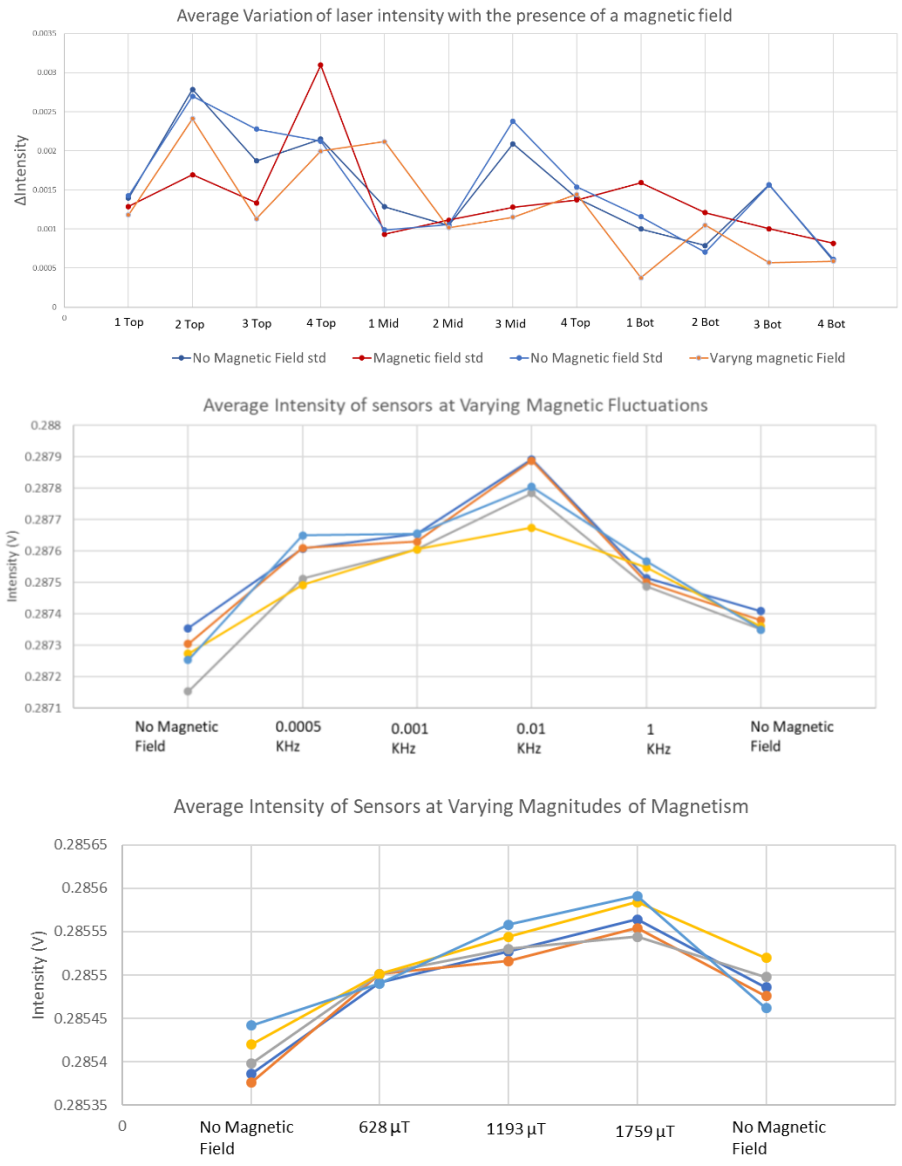

Fig.4

Similar to the previous experiment, the increased intensity of the magnetic field resulted more dissipation of water vapor, resulting higher intensity in each array of lasers. several measures were taken to avoid/attenuate the effects of electromagnetism radiation in the surrounding area. The experiment was taken place in a dark room with the setup completely covered by a faraday cage. Even though, the magnetic field measured within the coil was 58 µT – 141 µT, the ambient field generated outside of the coil and within the tank was observed to be lower than it (25 µT<B< 80 µT). This suggest that, the experiment induced the water molecules within the tank a magnetic field somewhat similar to the geomagnetic field strength of earth.

Conclusion

This study could contribute to distinguishing between natural climate variability and how it is altered by anthropogenic causes. Further investigations are necessary to further investigate the underlying cause of the experimental variation. The knowledge gained through this study serves as an important starting point to further investigate the effects of geomagnetic fluctuations on water vapor variability. Currently, a study is being conducted to identify temporal variations in the atmospheric water vapor caused by fluctuations in the earth's geomagnetism.

References

Annalisa Dalmoro, Anna Angela Barba, and Matteo d'Amore, "Analysis of Size Correlations for Microdroplets Produced by Ultrasonic Atomization," The Scientific World Journal, vol. 2013, Article ID 482910, 7 pages, 2013.

H. Svensmark, E. Friis-Christensen, Variation of cosmic ray flux and global cloud coverage — a missing link in solar–climate relationships, J. Atmos. Sol. -Terr. Phys. 59 (1997) 1225–1232.

J.E. Kristjansson, J. Kristiansen, E. Kaas, Solar activity, cosmic rays, clouds and climate . Adv. Space Res. 34 (2004) 407–415.

W.F. Ruddiman, Earth's Climate: Past and Future, 2nd ed., W.H. Freeman and Co, New York, 2002

Y. Guyodo, J.P. Valet, Global changes in intensity of the Earth's magnetic field during the past 800 kyr, Nature 399 (1999) 249–252.

Name: Reid Roberson
Major: Mathematics
Faculty Mentor, Department: Dr. Shantia Yarahmadian, Mathematics

Comparing Ancient and Modern Cosmology

At the beginning of this project the stated goal was to examine the connection between ancient and modern cosmologies. A series of questions was presented: Are ancient philosophies and modern observations compatible? Does the application of ancient philosophies to modern observations change our interpretations significantly? Do modern philosophies adequately support modern observations? Are ancient philosophies still worth examining even if they unsatisfactorily align with modern observations? I made the claim that if any of these questions were answered, the project could be considered successful.

As we progressed, it became clear that some of these questions were unanswerable. The primary reference for ancient cosmological ideas in the project is Plato's *Timaeus.* What study of this work revealed is that scientific study and method of the past is in a completely different realm than that of the scientific study and method of today. Plato's work presents a vivid creation story that connects music and art and biology and astronomy; he describes how he sees our world quilted together out of these pieces. The modern work contrasted against Plato is Andrew Liddle's *An Introduction to Modern Cosmology.* While this book does an incredible job of presenting the modern science of cosmology, its content is clinical and observation driven. Respected cosmologist Steven Weinberg talks of how cosmology was an ignoble pursuit in the 1950's, not the sort of thing to which a "respectable scientist would devote his time." Clearly, this has changed, but only after the less 'scientific' aspects of cosmology were culled from the discipline.

For me, this is an interesting dilemma as it places me very much in the role of a philosopher rather than a scientist. In fact, the third major work studied throughout the project was Rene Guenon's *The Multiple States of Being*. (Guenon was certainly a philosopher, and not a scientist.) It was quite an enlightening and unusual experience to study so broadly, and I feels it hearkens back to the ancient way of doing things.

A more comprehensive presentation is being prepared for the spring, but at least one of the original questions has been answered. Are ancient philosophies still worth examining even if they unsatisfactorily align with modern observations? It seems that they can serve two major purposes. First, study of ancient ideas puts modern ideas in context and offers due respect the the thinkers of the past, and, second, ancient ideas are still tied up in good philosophy even if the science is imperfect.

I would like to thank Dr. Yarahmadian for his guidance and encouragement and patience as I worked through some of the texts. I would also like to thank Dr. Oppenheimer and the Honors College for facilitating this wonderful opportunity.

Robust Positioning for Autonomous Platforms Using Adaptive Measurement Noise Covariance Distributions

Jacob A. Rogers*, Aerospace Engineering
Mississippi State University, Mississippi State, MS, 39759

Faculty Mentor, Department: Donghoon Kim, PhD, Aerospace Engineering

This paper is predominately concerned with the development of a low cost and accurate sensing system for autonomous platforms that operate indoors and in locations impenetrable by GPS signal. The indoor positioning system (IPS) discussed in this paper uses ultra-wide band (UWB) ranging sensors to provide distance measurements needed for trilaterating the position of objects. Without any research and modification, the UWB can only estimate objects' position within ten centimeters due to the measurements being corrupted by noise that greatly affects the ranging process. Under certain circumstances, such as encounters with metallic structures, the UWB ranging sensor can experience larger measurement noise. Using modified Kalman filter algorithms that possess updating measurement noise covariance matrices, the positioning unreliabilities caused by these abnormal interferences can be mitigated. Through simulation, both the nominal noise and random interference noise were reduced thus yielding accurate state estimates. By increasing the accuracy of the UWB sensors through this approach, the given IPS becomes a more stable and robust environment for localization.

I. Introduction

Accurate and reliable indoor positioning systems (IPSs) are currently a significant topic of research due to their broad applications. Whether navigating blind individuals through public areas or providing positioning information to an unmanned autonomous vehicle (UAV), more accurate IPSs could augment the daily lives of countless individuals. An IPS operates by using distance information from various ranging sensors to trilaterate the position of an object or user. Depending on the functionality of the sensor being used, IPSs can provide either two-dimensional or three-dimensional positioning in real-time. To date, IPSs have been constructed and implemented, but usually these systems provide information that is not reliable enough for many applications especially in dynamic situations. In attempting to find solutions, researchers have applied multiple diverse techniques, such as comparing the performance of various ranging sensors.

Among the many ranging sensors available today, ultra-wideband (UWB) technology has become a popular research topic within the past decade due to approval from the Federal Communications Commission (FCC) for commercial use in 2002. Localization is currently among the most popular uses for this technology. Ranging sensors using UWB technology often outperform many of the competing ranging sensors due to their distinctive characteristics, such as multi-path resistance and low power consumption. Although these sensors remain a strong competitor without major modification, they are still rife with measurement noise. In addition to the nominal noise, UWB ranging sensors experience much larger measurement errors when interfered by metallic structures or other threatening objects. These unanticipated errors destabilize localization, especially if the tracked object is dependent upon the positioning for active navigation.

In previous work, many attempts have been made to apply computational methods to UWB ranging sensors in order to reduce measurement noise. A comparison of various methods can be found in Ref. [1]. More specifically in Ref. [2], Banerjee discusses a way to improve the accuracy of UWB measurements through noise modeling and particle filtering. When considering the measurement noise covariance estimation, the research broadens to more general systems. In Ref. [3], Assa and Plataniotis assume that the measurement and process noise covariance distributions are not known *a prior* and used a Kalman filter algorithm to converge to the distribution through finite sampling, and Nguyen and Guillemin have a similar approach in Ref. [7] specifically for process noise using least squares. Likewise, Ref. [8] presents how Nguyen et al. estimate both noise covariance distributions using the innovative and residual errors. After providing

*Student and Undergraduate Researcher, Department of Aerospace Engineering, 330 Walker Hardy Rd, Mississippi State, MS 39762

a confirmation as to why standard joint estimation is unsuitable for noise covariance matrix estimation, Dunik et al. compare and analyze third-order parameter estimation and one-step and multi-step prediction error based correlation methods in Ref. [9]. To the best of the authors knowledge, the papers concerning noise reduction and measurement noise covariance matrix updating lack a) measurements that are corrupted by random interferences additional to the nominal noise and b) a measurement noise covariance that intentionally updates at every time step to account for said interferences.

This paper discusses possible methods to mitigate not only the expected noise but also the unexpected interferences through two measurement noise covariance adaptive techniques introduced in this paper. The two filtering algorithms are applied to dynamic measurements recorded from commercial UWB ranging sensors. Since dynamic scenarios are of much greater concern for actively tracking objects, the majority of this paper discusses noise reduction and state estimation for objects (or users) in motion. Therefore a dynamic simulation is formulated where the measured values are corrupted by nominal noise plus a random interference to imitate a sensor's encounter with metallic structures. Ultimately, to accurately estimate the position of the tracked object despite the unexpected noise, a Kalman filter (KF) algorithm was applied. Section (II) provides the background information on UWB ranging sensor technology, indoor positioning, and traditional discrete-time computational filtering necessary to understand the material presented in this work. Section (III) introduces the two new approaches to mitigating errors when random interference occur. To proceed, Sec. (IV) provides the simulation formulation needed to obtain the results presented in Sec. (V). Ultimately, conclusion are drawn from the contents of this paper in Sec. (VI).

II. Background

A. UWB Ranging

Although UWB technology has a variety of functions, the more developed concept of the technology has two distinct research areas: short range communication with high data rates and localization applications. This paper focuses specifically on the technology's ranging capability and its role in the IPS. Among the many characteristics that make it a suitable ranging sensor, UWB is known in the localization research area for its high data rates, low power consumption, accurate positioning, and resistance to multipath interference. The FCC, the primary regulatory body for UWB, defines the technology as a wireless system with a bandwidth that is greater than 500 MHz; however, positioning operations must reside between 3.1 and 10.6 GHz [10]. Discussions on the FCC regulations can be found in Refs. [11] and [12]. Comparisons between UWB ranging technology and other competing technologies is presented in Refs. [13] and [14].

Moving on from the traits that characterize UWB technology, ranging sensors that utilize UWB take advantage of the known speed of radio wave propagation, which is the speed of light c. When using time of arrival (TOA) to approximate the range, the distance between two nodes can be theoretically found by multiplying the speed of light by the time difference between transmission and reception, meaning that the node-to-node distance is directly proportional to the radio signal propagation time [15], [16]. For TOA to work, the nodes must possess common clocks. Considering this, the theoretical range between two nodes can generally be expressed as

$$d_i = c(t_\mathrm{r} - t_\mathrm{t}) \tag{1}$$

where d_i is the i^{th} distance between two nodes and t_r and t_t are the reception and transmission times, respectively.

This concept can be physically represented in two-dimensions, with the estimated range forming a circle. The word "estimated" is used to reflect that the range calculation is only theoretically perfect due to the speed of light changing for different environmental features. Figure 1 depicts a two-dimensional (2D) representation of the ranging estimation process. Applying this concept when there are three stationary nodes and one target node allows for what is commonly known as trilateration. *Trilateration* is a form of triangulation that uses distances between reference points to estimate object positions. This topic serves as the foundation for indoor positioning [17].

B. Indoor Positioning

While positioning with ranging sensors is not limited to indoor applications, this paper primarily focuses on the improvement of an IPS. Positioning is simply defined as the concept of locating objects or users using sensors such as cameras, ultrasonics, or UWB radio signals. Due to primary progress being made within the last decade, IPSs have

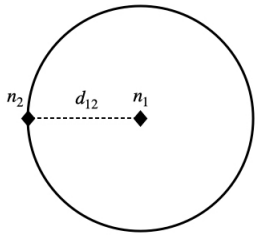

Fig. 1 2D depiction of ranging estimate.

increased in popularity and attained strong interests within both civilian and militaristic communities due to the system's broad range of applications. A few current applications consist of: tracking products within a warehouse, providing the position of firemen inside a burning building, enabling military personnel to accurately track soldiers within an enclosed structure, and assisting autonomous vehicles with reliable position data. According to Ref. [18], benchmarking can be performed for a given IPS based on its accuracy, precision, complexity, robustness, scalability, and cost. For the IPS discussed in this work, accuracy and robustness are the primary benchmarks of concern for improvement. An IPS's *accuracy* is commonly measured by the system's mean distance error: the difference between the average estimated location and the true location. The robustness of an IPS describes how well the system performs under abnormal conditions.

Before discussing how an IPS operates, some terminology must be introduced. These terms vary across literature, but the concept remains unchanged. For the IPS constructed in this research, there are two classifications for nodes: an anchor and a tag. An *anchor* is a stationary UWB ranging sensor that has a manually set position in three-dimensional space. The UWB ranging sensor attached to the object or user begin tracked is referred to as a *tag*.

To estimate the position of tag in space, at least three anchors are needed. Two anchors theoretically produce two circles that intersect at two different points while the addition of a third anchor creates three circles that intersect at one point. From rudimentary mathematics, the distance between two points in space (or between one anchor and one tag) can be represented as

$$d_{i_k} = \sqrt{(\mathbf{s}_i - \mathbf{x}_k)^T (\mathbf{s}_i - \mathbf{x}_k)} \tag{2}$$

where $\mathbf{s}_i = [s_x \quad s_y]_i^T$ is the static position of the i^{th} anchor and $\mathbf{x}_k = [x \quad y]_k^T$ is the tag's position corresponding to the k^{th} time step. The z position is not considered here due to only the x and y being of concern for application, but it can easily be implemented.

For the IPS discussed, there are three anchors, each providing a distance measurement. Although only the x and y position are considered, three distances are required to calculate the position of the tag. Taking into account the three anchor measurements, two additional distance equations arise to give three total equations expressed as

$$d_{1_k} = \sqrt{(\mathbf{s}_1 - \mathbf{x}_k)^T (\mathbf{s}_1 - \mathbf{x}_k)} \tag{3a}$$

$$d_{2_k} = \sqrt{(\mathbf{s}_2 - \mathbf{x}_k)^T (\mathbf{s}_2 - \mathbf{x}_k)} \tag{3b}$$

$$d_{3_k} = \sqrt{(\mathbf{s}_3 - \mathbf{x}_k)^T (\mathbf{s}_3 - \mathbf{x}_k)} \tag{3c}$$

Using these equations, the position $\mathbf{x}_k$ can be trilaterated for each measurement. In real-time, the position of the tag can be calculated in various ways, such as linearizing Eq. 3, [19], or applying a least square approach. Although this work only considers the 2D positioning, three distance equations are needed because one of the equations is substituted into the others to linearize the system for the real-time calculations. It is important to note that trilateration yields values that are often highly inaccurate due to the direct use of raw distance measurements. With this in mind, the 2D representation of the positioning system is refined in Fig. 2.

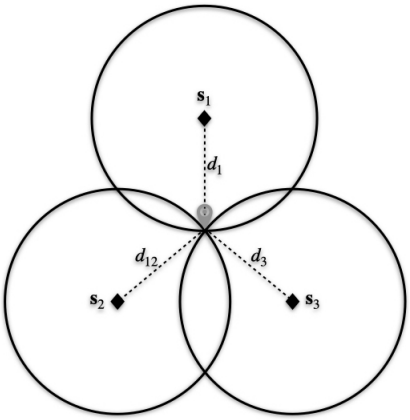

Fig. 2 2D depiction of ranging for positioning system.

C. Discrete-Time Kalman Filter

The KF has been proven to be efficient in linear dynamic situations. Since the ultimate goal is to more accurately track moving autonomous platforms, the KF is more appealing. The UWB ranging sensors provide distance measurements at a fixed update rate making them ideal for the discrete-time KF. Although distances are the actual measurements received from the sensors, the assumption is made that the post-trilateration x and y position is the measurement. This makes modeling dynamic simulation (discussed in Section IV) much simpler. The following expressions for the KF are referenced from Ref. [4].

The KF algorithm estimates a system's state by predicting the *a prior* estimate and then updating this prediction after taking into consideration the measurements to ultimately obtain the *a posterior* estimate. The noise corrupting the UWB ranging sensor measurements is similar to white noise, so for this discussion, the model and measurements are disturbed by zero-mean Gaussian white-noise. The "truth" model for a given system is expressed in Eq. 4.

$$\mathbf{x}_{k+1} = \mathbf{\Phi}_k \mathbf{x}_k + \mathbf{\Gamma}_k \mathbf{u}_k + \mathbf{\Upsilon}_k \mathbf{w}_k \tag{4a}$$

$$\tilde{\mathbf{y}}_k = \mathbf{H}_k \mathbf{x}_k + \mathbf{v}_k \tag{4b}$$

where $\mathbf{\Phi}_k$ is the state transition matrix, $\mathbf{\Gamma}_k$ is the control matrix, $\mathbf{u}_k$ is the control vector, $\mathbf{\Upsilon}_k$ is the process noise matrix, $\mathbf{w}_k \sim N(\mathbf{0}, \mathbf{Q}_k)$ is the process noise vector, $\mathbf{H}_k$ is the observation matrix, $\mathbf{v}_k$ is the measurement noise, and $\mathbf{R}_k$ and $\mathbf{Q}_k$ are the measurement error covariance matrix and process error covariance matrix, respectively.

To start the algorithm, the filter must be provided a state estimate for initialization. These values will be updated with each iteration of the KF, ideally approaching the true values. The initial state is commonly expressed as

$$\hat{\mathbf{x}}(t_0) = \hat{\mathbf{x}}_0 \tag{5a}$$

$$\mathbf{P}_0 = E\{\tilde{\mathbf{x}}(t_0)\tilde{\mathbf{x}}^T(t_0)\} \tag{5b}$$

where $\hat{\mathbf{x}}(t_0)$ indicates the initial state estimate, $\mathbf{P}_0$ is the initial state error covariance matrix, and $\tilde{\mathbf{x}}(t_0)$ is the initial measurement error covariance.

During each iteration, the predicted state propagation (Eq. 5 for the first iteration) is updated based on the measurements. Before updating, the Kalman gain must be calculated. The Kalman gain essentially determines how much to weigh the current measurement value. If the measurementd seem unreliable, the gain puts less weight on the measurement values, making the state estimation more reliant on the prediction. The Kalman gain is given by

$$\mathbf{K}_k = \mathbf{P}_k^- \mathbf{H}_k^T [\mathbf{H}_k \mathbf{P}_k^- \mathbf{H}_k^T + \mathbf{R}_k]^{-1} \tag{6}$$

where $\mathbf{H}_k$ is the observation matrix and $\mathbf{P}_k^-$ is the *a prior* state error covariance matrix.

Once the Kalman gain has been calculated, the *a posterior* state estimate and state error covariance matrix can be calculated. This is the updated estimate that will be returned by the KF. With each iteration of the KF, the state estimate is updated using Eqs. 17.

$$\hat{\mathbf{x}}_k^+ = \hat{\mathbf{x}}_k^- + \mathbf{K}_k[\tilde{\mathbf{y}}_k - \mathbf{H}_k\hat{\mathbf{x}}_k^-] \tag{7a}$$

$$\mathbf{P}_k^+ = [\mathbf{I} - \mathbf{K}_k\mathbf{H}_k]\mathbf{P}_k^- \tag{7b}$$

where $\hat{\mathbf{x}}_k$ is the k^{th} *a posterior* state estimate, $\tilde{\mathbf{y}}_k$ is the state measurement, and $\mathbf{P}_k^+$ is the *a posterior* state error covariance matrix.

With every iteration, the KF predicts the next *a prior* estimate based on the current *a posterior* estimate. This prediction is accomplished by multiplying the estimate and the state transition matrix, which is formulated using the system model. As stated, this propagation is known as the *a prior* estimate. The equations used to propagate the prediction for the next Kalman iteration are given by

$$\hat{\mathbf{x}}_{k+1}^- = \mathbf{\Phi}_k\hat{\mathbf{x}}_k^+ + \mathbf{\Gamma}_k\mathbf{u}_k \tag{8a}$$

$$\mathbf{P}_{k+1}^- = \mathbf{\Phi}_k\mathbf{P}_k^+\mathbf{\Phi}_k^T + \mathbf{\Upsilon}_k\mathbf{Q}_k\mathbf{\Upsilon}_k^T \tag{8b}$$

Most traditional variations of the KF algorithm make the assumption that the measurement noise covariance is constant. In theory, this assumption could be applicable under circumstances where the measurement noise remains nominal (i.e. does not exceed the expected standard deviation). If the measurements are randomly interfered causing the standard deviation to be abnormal, the methods where the measurement noise covariance is constant become unreliable. By updating the measurement error covariance matrix, this uncertainty in the state estimate caused by unanticipated interference can be reduced.

III. Interference Adaptive Approaches

Since UWB sensors are highly susceptible to random interference from metallic structures and other materials, the KF with a constant measurement noise covariance can be inadequate. For sensors that possess rather steady, or predictable, noise, the constant noise covariance works as intended. The KF algorithm is modified to account for these random interferences by updating the measurement noise covariance in a recursive manner using the measurement noise covariance shift (MNCS) or the measurement noise covariance batch (MNCB) approach. Through simulation and experimental results, these modifications are compared and proven superior to the KF with a constant measurement noise covariance. The state of the system when using the modified KF is principally unchanged and still evolves in accordance with the discrete-time dynamic model introduced in Eq. 4 for both adaptive methods.

A. MNCB Technique

One way to increase the performance of the KF in uncertain noise scenarios is to implement the MNCB adaptive method into the traditional KF. The MNCB approach allows the KF to adapt to the noise by updating the measurement noise covariance matrix after a certain number of measurements have been collected. These measurements are referred to in this work as a *batch*, and the amount of measurements in a batch are indicated by N_b. Depending on the dynamic situation, N_b can be tuned to increase the performance of the MNCB KF. Since the measurement noise covariance is intentionally changing with time, it will be indicated by $\hat{\mathbf{R}}$ rather than $\mathbf{R}$ to clearly distinguish the constant and adaptive methods.

If the system is modeled as Eq. 4 and $\hat{\mathbf{x}}_0$ and $\hat{\mathbf{P}}_0$ are initialize as Eq. 5, then the initial measurement error covariance matrix can be expressed as

$$\hat{\mathbf{R}}_0 = \mathbf{I}_n \sigma^2 \tag{9}$$

where $\mathbf{I}_n$ is the nxn identity matrix, n is the number of states, and σ is the nominal (expected) measurement standard deviation.

It is important to note that the MNCB approach does not provide an estimate corresponding to every measurement. After N_b measurements, the measurement error covariance can be calculated as

$$\hat{\mathbf{R}}_k^i = \mathrm{cov}(\tilde{\mathbf{y}}_{k-N_\mathrm{b}:k}) \tag{10}$$

where i indicates the i^{th} MNCB estimate corresponding to the k^{th} time step and $\mathrm{cov}(\boldsymbol{\alpha})$ represents the $n \times n$ covariance matrix for generic vector $\boldsymbol{\alpha}$. This is due to the MNCB algorithm providing an estimate only after every N_b measurements, so if k measurements are provided, k/N_b states will be estimated.

The remaining expressions of the KF are unchanged. After the measurement noise covariance has been updated, the Kalman gain can be calculated as

$$\mathbf{K}_k^i = \mathbf{P}_k^{i-}\mathbf{H}_k^T[\mathbf{H}_k\mathbf{P}_k^{i-}\mathbf{H}_i^T + \hat{\mathbf{R}}_k^i]^{-1} \tag{11}$$

Similarly to Eq. 17, the i^{th} state update corresponding to the k^{th} time step can be updated by implementing the MNCB method. The state update equations become

$$\hat{\mathbf{x}}_k^{i+} = \hat{\mathbf{x}}_k^{i-} + \mathbf{K}_k^i[\tilde{\mathbf{y}}_k - \mathbf{H}_k\hat{\mathbf{x}}_k^{i-}] \tag{12a}$$

$$\mathbf{P}_k^{i+} = [\mathbf{I}_n - \mathbf{K}_k^i\mathbf{H}_k]\mathbf{P}_k^{i-} \tag{12b}$$

and lastly the state prediction equations can be expressed as

$$\hat{\mathbf{x}}_{k+1}^{i-} = \boldsymbol{\Phi}_k\hat{\mathbf{x}}_k^{i+} + \boldsymbol{\Gamma}_k\mathbf{u}_k \tag{13a}$$

$$\mathbf{P}_{k+1}^{i-} = \boldsymbol{\Phi}_k\mathbf{P}_k^{i+}\boldsymbol{\Phi}_k^T + \boldsymbol{\Upsilon}_k\mathbf{Q}_k\boldsymbol{\Upsilon}_k^T \tag{13b}$$

The MNCB algorithm provides a way to account for unexpected changes in the measurement noise but with limitations. For example, it does not provide an estimate at every measurement time step. This can be problematic for sensors with low sampling frequencies. However, for sensors with a relatively high update rate, this approach can yield better results, especially for the case when a random interference is encounter by said sensors. Algorithm 1 presents a summarized version of the MNCB method for brevity.

B. MNCS Technique

When compared to the MNCB approach, the MNCS method resolves the update problem by modifying the algorithm to *shift* the batch rather than obtain a new batch every N_b measurements. The shifting batch size is indicated by N_s to avoid confusion. This approach operates by dropping the last batch measurement and adding the current measurement, always keeping a constant N_s measurements in the shifting batch.

As for the MNCB method, this technique is assuming a model in accordance with Eq. 4. Also, $\hat{\mathbf{x}}_0$ and $\hat{\mathbf{P}}_0$ are initialize as Eq. 5. Since the MNCS approach requires at least N_s measurements to begin, the first N_s measurement noise covariance matrices are given as

$$\hat{\mathbf{R}}_k = \mathbf{I}_n \sigma^2 \tag{14}$$

where σ is the nominal standard deviation characteristic of a UWB ranging sensor.

After N_s measurements have been acquired, the algorithm can begin updating the measurement noise covariance matrix. The expression switches from a constant matrix to

Algorithm 1 MNCB Adaptation Technique

Inputs: $\mathbf{\Phi}_k$, $\mathbf{\Upsilon}_k$, $\mathbf{\Gamma}_k$, $\mathbf{H}_k$, $\mathbf{Q}_k$, N_b, $\hat{\mathbf{R}}_0$, $\hat{\mathbf{x}}_0$, $\mathbf{P}_0$, $\tilde{\mathbf{y}}_k$
$j = 0, i = 0$
for $k = 1 : T_{\max}$ **do**
    $j = j + 1$
    if $j = N_\mathrm{b}$ **do**
        Update $\hat{\mathbf{R}}$:
        $i = i + 1$
        $\hat{\mathbf{R}}_k^i = \mathrm{cov}(\tilde{\mathbf{y}}_{k-N_\mathrm{b}:k})$
        $\mathbf{K}_k^i = \mathbf{P}_k^{i-}\mathbf{H}_k^T[\mathbf{H}_k\mathbf{P}_k^{i-}\mathbf{H}_k^T + \hat{\mathbf{R}}_k^i]^{-1}$
        State Update:
        $\hat{\mathbf{x}}_k^{i+} = \hat{\mathbf{x}}_k^{i-} + \mathbf{K}_k^i[\tilde{\mathbf{y}}_k - \mathbf{H}_k\hat{\mathbf{x}}_k^{i-}]$
        $\mathbf{P}_k^{i+} = [\mathbf{I}_n - \mathbf{K}_k^i\mathbf{H}_k]\mathbf{P}_k^{i-}$
        Predict Next State:
        $\hat{\mathbf{x}}_{k+1}^{i-} = \mathbf{\Phi}_k\hat{\mathbf{x}}_k^{i+} + \mathbf{\Gamma}_k\mathbf{u}_k$
        $\mathbf{P}_{k+1}^{i-} = \mathbf{\Phi}_k\mathbf{P}_k^{i+}\mathbf{\Phi}_k^T + \mathbf{\Upsilon}_k\mathbf{Q}_k\mathbf{\Upsilon}_k^T$
        $j = j - N_\mathrm{b}$
    end if
end for

$$\hat{\mathbf{R}}_k = \mathrm{cov}(\tilde{\mathbf{y}}_{k-N_\mathrm{s}:k}) \tag{15}$$

and the Kalman gain for the MNCS method is

$$\mathbf{K}_k = \mathbf{P}_k^-\mathbf{H}_k^T[\mathbf{H}_k\mathbf{P}_k^-\mathbf{H}_k^T + \hat{\mathbf{R}}_k]^{-1} \tag{16}$$

Following directly from the traditional KF, the *a posterior* state estimate accounting for the updating noise covariance matrix becomes

$$\hat{\mathbf{x}}_k^+ = \hat{\mathbf{x}}_k^- + \mathbf{K}_k[\tilde{\mathbf{y}}_k - \mathbf{H}_k\hat{\mathbf{x}}_k^-] \tag{17a}$$

$$\mathbf{P}_k^+ = [\mathbf{I} - \mathbf{K}_k\mathbf{H}_k]\mathbf{P}_k^- \tag{17b}$$

and the predicted state is propagated by

$$\hat{\mathbf{x}}_{k+1}^- = \mathbf{\Phi}_k\hat{\mathbf{x}}_k^+ + \mathbf{\Gamma}_k\mathbf{u}_k \tag{18a}$$

$$\mathbf{P}_{k+1}^- = \mathbf{\Phi}_k\mathbf{P}_k^+\mathbf{\Phi}_k^T + \mathbf{\Upsilon}_k\mathbf{Q}_k\mathbf{\Upsilon}_k^T \tag{18b}$$

Using this method, the algorithm can estimate the state every k^{th} time step by eliminating the $k^{\mathrm{th}} - N_\mathrm{s}$ measurement and obtaining the k^{th}. As for N_b, N_s can be tuned for the best results for any given system. By constantly updating the measurement noise covariance matrix, the KF is better prepared to confront unexpected obstructions and adapt to changing noise levels thus providing less error in the state estimates. A condensed version of the MNCS approach is provided in Algorithm 2.

Algorithm 2 MNCS Adaptation Technique

Inputs: $\mathbf{\Phi}_k$, $\mathbf{\Upsilon}_k$, $\mathbf{\Gamma}_k$, $\mathbf{H}_k$, $\mathbf{Q}_k$, N_s, $\hat{\mathbf{R}}_0$, $\hat{\mathbf{x}}_0$, $\mathbf{P}_0$, $\tilde{\mathbf{y}}_k$
for $k = 1 : T_\text{max}$ **do**
    Update $\mathbf{R}$:
    if $k \leq N_\text{s}$ **do**
        $\hat{\mathbf{R}}_k = \mathbf{I}_n \sigma^2$
    else do
        $\hat{\mathbf{R}}_k = \text{cov}(\tilde{\mathbf{y}}_{k-N_\text{s}:k})$
    end if
    $\mathbf{K}_k = \mathbf{P}_k^- \mathbf{H}_k^T [\mathbf{H}_k \mathbf{P}_k^- \mathbf{H}_k^T + \hat{\mathbf{R}}_k]^{-1}$
    State Update:
    $\hat{\mathbf{x}}_k^+ = \hat{\mathbf{x}}_k^- + \mathbf{K}_k [\tilde{\mathbf{y}}_k - \mathbf{H}_k \hat{\mathbf{x}}_k^-]$
    $\mathbf{P}_k^+ = [\mathbf{I} - \mathbf{K}_k \mathbf{H}_k] \mathbf{P}_k^-$
    Predict Next State:
    $\hat{\mathbf{x}}_{k+1}^- = \mathbf{\Phi}_k \hat{\mathbf{x}}_k^+ + \mathbf{\Gamma}_k \mathbf{u}_k$
    $\mathbf{P}_{k+1}^- = \mathbf{\Phi}_k \mathbf{P}_k^+ \mathbf{\Phi}_k^T + \mathbf{\Upsilon}_k \mathbf{Q}_k \mathbf{\Upsilon}_k^T$
end for

IV. Dynamic Simulation Methodology

This section steps through the formulation of the dynamic simulation and the parameters used in the simulation, itself. The simulation was created in MATLAB as well as the filtering algorithms. To actively evaluate the algorithm's significance, two simulations are constructed to represent both the *nominal* positioning by UWB ranging sensors and *interfered* positioning by equivalent sensors. The performances of the traditional, MNCB, and MNCS KFs are analyzed and compared for the two measurement noise scenarios.

Since the unmodified KF solely applies to linear systems, the simulation was modeled to be linear. With this in mind, the dynamic system model consists of a tag moving at a constant velocity in a linear path. Following from Eq. 4, the dynamic system for two states x and y was modeled as

$$\mathbf{x}_{k+1} = \mathbf{\Phi} \mathbf{x}_k + \mathbf{\Gamma} \mathbf{u} + \mathbf{\Upsilon}_k \mathbf{w}_k \tag{19}$$

where $\mathbf{x}_k = [x \quad y]_k^T$, $\mathbf{\Phi} = \mathbf{I}_2$ is constant, $\mathbf{\Gamma} = \mathbf{I}_2 \Delta t$ is constant with $\Delta t = 0.1$ s, $\mathbf{u} = [v_x \quad v_y]^T$ is constant with v_x and v_y both 0.1 m/s, $\mathbf{\Upsilon} = \mathbf{I}_2$, $\mathbf{w}_k = \sigma_\text{p} \mathbf{randn}(2,1)$, and $\sigma_\text{p} = 10e - 5$ m.

The measurement values are assumed to be corrupted by zero-mean Gaussian white noise. Depending on the simulation method, the noise is either nominal or interfered. For the *nominal* case, the x and y measurement values are propagated as

$$\tilde{\mathbf{y}}_k = \mathbf{H} \mathbf{x}_k + \mathbf{v}_{\text{nom},k} \tag{20}$$

where $\tilde{\mathbf{y}}_k = [\tilde{y}_x \quad \tilde{y}_y]_k^T$ is the k^th x and y measurements, $\mathbf{H} = \mathbf{I}_2$, $\mathbf{v}_{\text{nom},k} = \sigma_\text{nom} \mathbf{randn}(2,1)$ is the nominal noise term, and $\sigma_\text{p} = 0.09$ m is the measurement standard deviation under nominal noise conditions.

If the UWB ranging sensors encounter some interferences, the measurement noise increases. To imitate this abnormal interference, the simulation increases the noise for a given time interval. This increase in measurement noise is simulated by

$$\tilde{\mathbf{y}}_k = \mathbf{H} \mathbf{x}_k + \mathbf{v}_{\text{int},k} \tag{21}$$

where $\mathbf{v}_{\text{int},k} = \sigma_\text{int} \mathbf{randn}(2,1)$ is the abnormal noise term and $\sigma_\text{int} = 0.50$ m. After the disturbance time interval is over, the noise term returns to the nominal state.

Moving forward, the simulation directly follows the KF algorithms given in Sects. (II.C), (III.A), and (III.B). The initial conditions and remaining parameters for the filters were set as

$$\mathbf{x}_0 = [1 \quad 1]^T \text{ m}$$

$$\mathbf{P}_0 = \mathbf{I}_2 \sigma_{\text{nom}}^2$$
$$\mathbf{R}_0, \hat{\mathbf{R}}_0 = \mathbf{I}_2 \sigma_{\text{nom}}^2$$
$$\mathbf{Q} = \mathbf{I}_2 \sigma_{\text{p}}^2$$

Using this discrete-time linear dynamic model, the simulation propagated the measurements (both nominal and interfered), the true position, and the estimates from each algorithm for a runtime of 30 seconds. Assuming that the simulation sensors have an update rate of 10 Hz, a runtime of 30 seconds yields 300 measurements making $k = 300$. The batch size for both MNCB and MNCS methods was set to 10. The simulation results are presented, compared, and analyzed in Sect. (V).

V. Dynamic Simulation Results

Continuing from Sec. (IV), this section displays and discusses the results from the two simulations. The significant differences between the nominal and interfered results are shown and compared. The comparison is necessary to validate that updating the measurement error covariance matrix improves the accuracy of the KF state estimations. The nominal and interfered scenarios are split into separate sections so the behavior and benefit of the MNCB and MNCS algorithms are clear.

A. Nominal Case

The dynamic system state trajectory using the aforementioned methods is displayed in Fig. 3 for the nominal case. All the time samples are shown in the figure. For the MNCB method, it is clear to see that there is only $i = k/N_{\text{b}} = 300/10 = 30$ estimates versus the 300 for the other approaches.

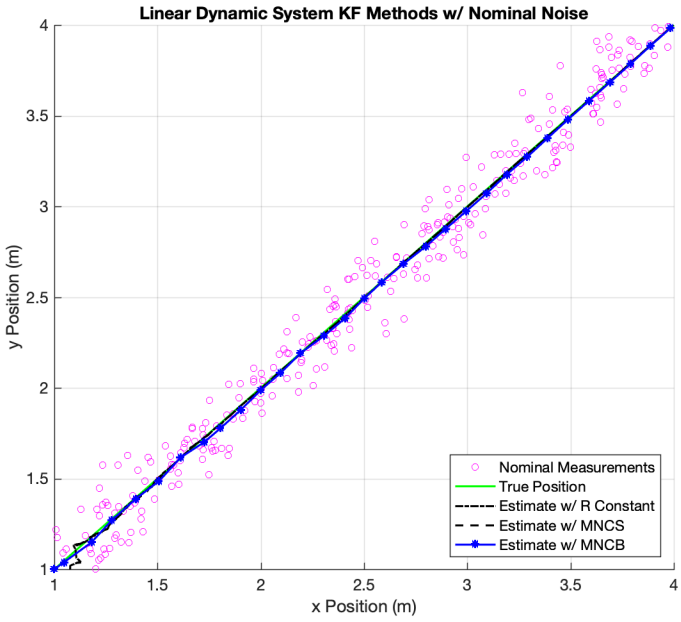

Fig. 3 State estimates for the nominal noise case.

One way to evaluate the KF estimator's performance it so analyze the *a posterior* estimate error. This estimate error can be defined as the difference between the true state measurement and the corresponding state e stimate. In reality, the true measurements are unknown, but for simulations, the real values can be determined. Figure 4 depicts the estimate errors for each aforementioned method along with their 3σ bounds.

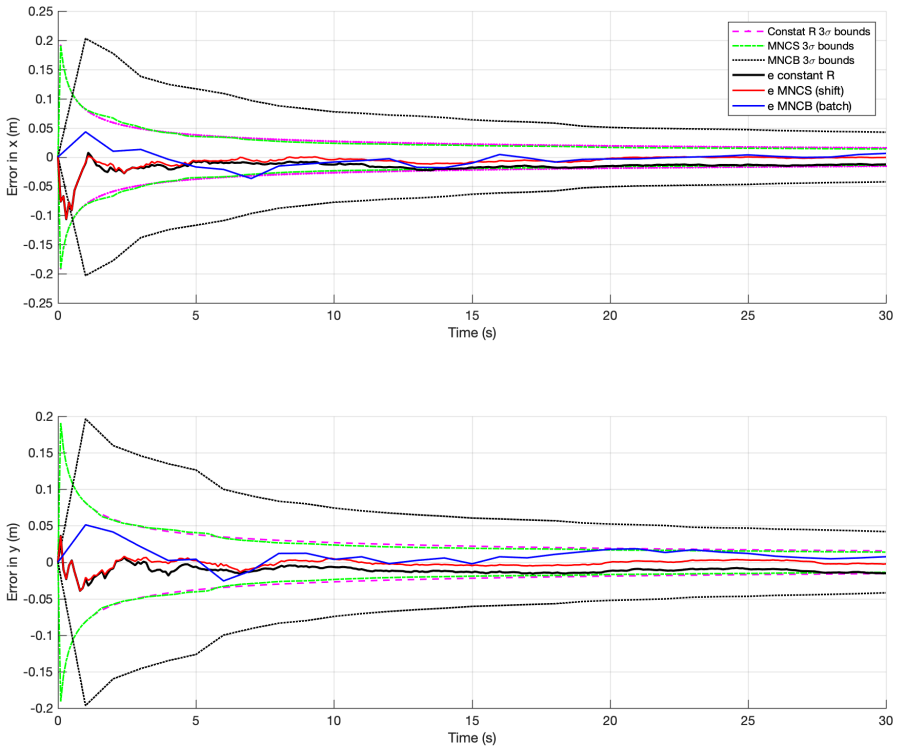

Fig. 4 State estimation errors plotted over time with 3σ bounds.

For the nominal case, none of the methods seem to outperform their counterparts (i.e. there seems to be no trend because the noise is as expected). The average values for the estimate errors are provide for each method in Table 1.

Table 1 Estimate errors over time for the *nominal* noise case.

Method	Constant **R**	MNCB	MNCS
$\tilde{e}_x^+$ (m)	0.0162	0.0090	0.0071
$\tilde{e}_y^+$ (m)	0.0115	0.0119	0.0040

With every i^{th} or k^{th} iteration, the measurement noise covariance updates to better adapt to the noise environment at an given time. To demonstrate how these distributions update, σ_x and σ_y corresponding to each method's measurement noise covariance matrix can be seen plotted of time in Fig. 5. This figure clearly shows how the matrix updates over time, excluding the traditional KF where the matrix remains constant with time.

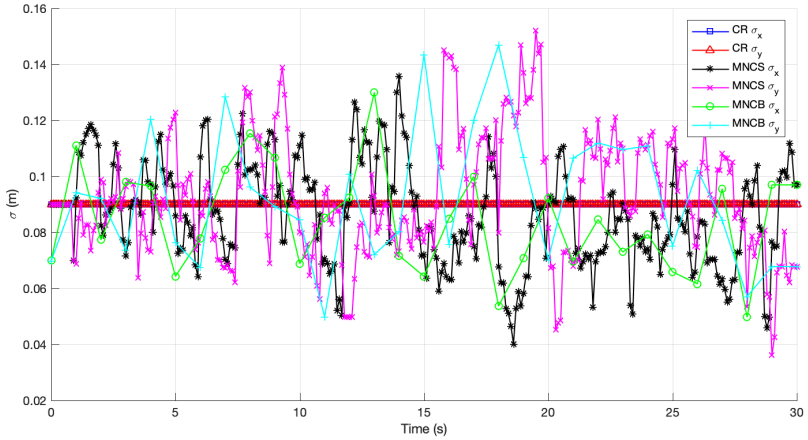

Fig. 5 Standard deviations of R as they update over time.

B. Interfered Case

When discussing the interfered case, the results get more interesting and the merit of the MNCS method is evident. For the simulation at hand, the random interference begins and ends at $t_1 = 12.5$ and $t_2 = 17.5$ seconds, respectively, allowing for 5 seconds of abnormal noise. As stated in Sect (IV), the standard deviation of the measurements during this time increases from $\sigma_{\text{nom}} = 0.09$ meters to $\sigma_{\text{int}} = 0.50$. The state estimate trajectories for each method as they respond to the disturbance are depicted in Fig. 6.

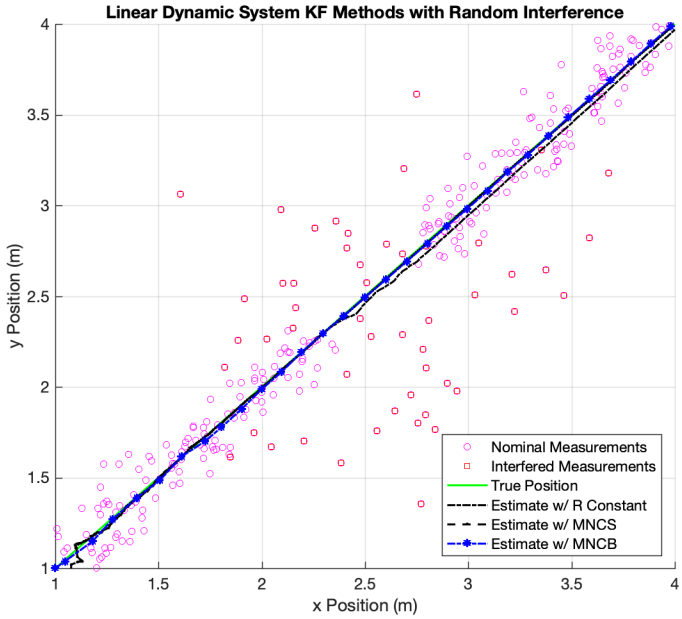

Fig. 6 State estimates for the interfered case.

The estimate errors provide even better representations of how various methods react to the abnormal interference. As for the nominal case, the reactions of the *a posterior* estimate errors can be seen plotted in Fig. 7.

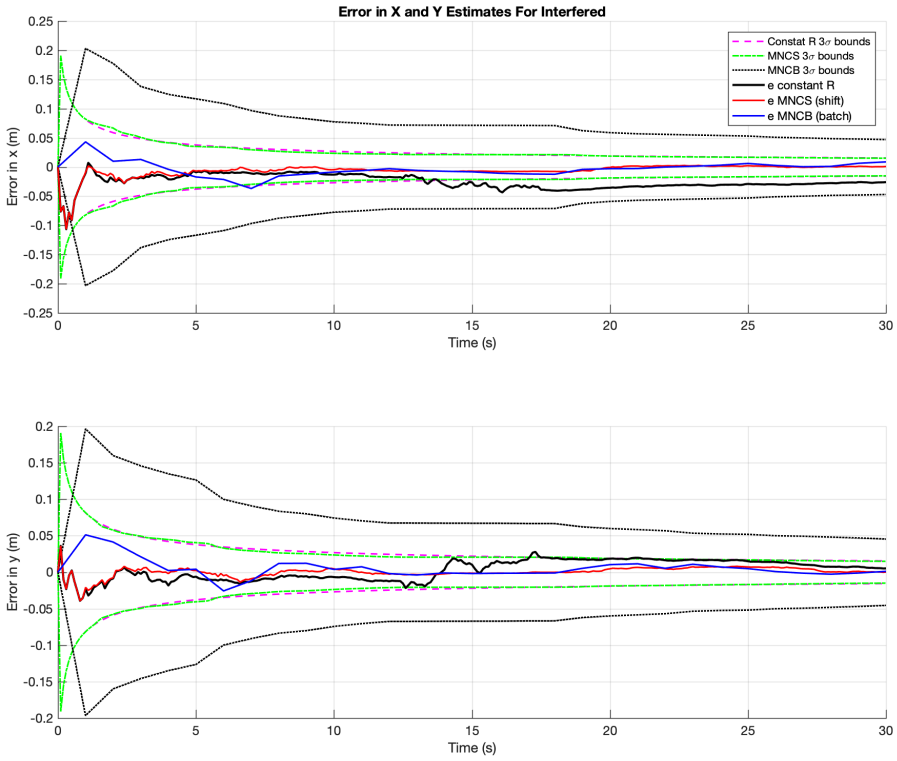

Fig. 7 State estimation errors plotted over time with 3σ bounds.

It is immediately clear that the traditional method performs poorly during the 5 second interference that it departs from its respective 3σ bounds. The MNCS approach seems to outperform the other two methods by providing the most accurate state estimations and almost being unaffected by the interference. Due to the updating nature of the MNCB approach, it takes longer to converge, but the estimate errors indicate that it too is unnoticeably affected by the disturbance. It is important to note that the MNCB has much wider bounds than the traditional and MNCS KF approaches. Table 2 gives the average estimate error for each method.

Table 2 Estimate errors over time for the *interfered* noise case.

Method	Constant **R**	MNCB	MNCS
$\tilde{e}_x^+$ (m)	0.0252	0.0092	0.0069
$\tilde{e}_y^+$ (m)	0.0125	0.0087	0.0043

Again, apart from the traditional method, the measurement noise covariance matrices update over time. Figure 8 is the similar to Fig. 5 but for the interfered case rather than the nominal. It is indisputable that the MNCB and MNCS measurement noise covariance matrices' σ_x and σ_y increase during the 5 second interference, allowing the modified KFs to account for the larger noise.

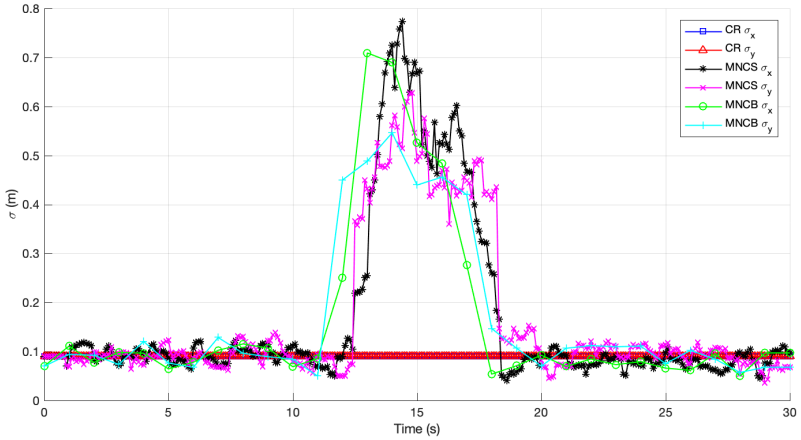

Fig. 8 Standard deviations of R as they update over time.

VI. Conclusion

Using the KF algorithms discussed in this paper, the position of a tracked object was more accurately estimated. The MNCS method seemed to out perform both the traditional (or constant) and MNCB KF. This is validated through the simulation of a common interference scenario experienced by UWB ranging sensors while also presenting the estimate errors for comparison. Moving forward, this algorithm can be implemented into an Extended Kalman filter (EKF) for better positioning in the nonlinear dynamic scenarios. Regardless, this is a significant step toward creating an affordable and robust IPS.

Acknowledgments

This work was made possible by the financial support of the Judy and Bobby Shackouls Honors College Summer Research Fellowship. I am especially appreciative of Dr. Donghoon Kim, assistant professor at Mississippi State University and advisor for this paper, for taking time from his career to provide unending assistance and guidance. He has never missed an opportunity to teach me and display, through example, the many characteristics of an exceptional researcher, and for this I am indebted to him. To accompany this assistance, Dr. Jichul Kim, Dr. Kim's postdoctoral researcher, selflessly coached me on the importance of hardware systems and always made sure that I thoroughly understood the hardware at hand. Ultimately, I would like to thank my fiancé, Hadley, for ceaselessly providing support and inspiration.

References

[1] Chóliz, J., Eguiábal, M., Hernández-Solana, A., and Valdovinos, A., "Comparison of Algorithms for UWB Indoor Location and Tracking Systems," *IEEE 73rd Vehicular Technology Conference*, 2011.

[2] Banerjee, S., "Improving Accuracy in Ultra-Wideband Indoor Position Tracking through Noise Modeling and Augmentation," *All Dissertations*, 2012.

[3] Assa, A., and Plataniotis, K. N., "Adaptive Kalman Filtering by Covariance Sampling," *IEEE Journal*, Vol. 24, No. 9, 2017, pp. 1288–1292.

[4] Crassidis, J. L., and Junkins, J. L., *Optimal Estimation of Dynamic Systems*, 2nd ed., Taylor & Francis Group, Boca Raton,FL, 2012, Chap. 3.

[5] Li, Q., Li, R., Ji, K., and Dai, W., "Kalman Filter and Its Application," IEEE, 2015.

[6] Welch, G., and Bishop, G., "An Introduction to the Kalman Filter," University of Carolina, 2006.

[7] Nguyen, H.-N., and Guillemin, F., "On process noise covariance estimation," *25th Mediterranean Conference on Control and Automation (MED)*, IEEE, 2017, pp. 1345–1348.

[8] Akhlaghi, S., Zhou, N., and Huang, Z., "Adaptive Adjustment of Noise Covariance in Kalman Filter for Dynamic State Estimation," Cornell University, 2017.

[9] Dunik, J., Šimandl, M., and Straka, O., "Methods for Estimating State and Measurement Noise Covariance Matrices: Aspects and Comparison," *IFAC Symposium on System Identification*, IFAC, Saint-Malo, France, 2009, pp. 372–377.

[10] Bellusci, G., *Ultra-Wideband Ranging for Low-Complexity Indoor Positioning Applications*, Delft University of Technology, Terlizzi, Italy, 2011.

[11] Martin, R. F., "Ultra-Wideband (UWB) Rules and Design Compliance Issues," *IEEE*, 2003, pp. 91–96.

[12] Wilzeck, A., Guirao, P., and Dimitrov, E., "UWB Technology and Regulation," wiseSense, 2018, pp. 1–23.

[13] Zafari, F., Gkelias, A., and Leung, K. K., "A Survey of Indoor Localization Systems and Technologies," 2018, pp. 1–30.

[14] Yassin, A., Nasser, Y., Awad, M., Al-Dubai, A., Liu, R., Yuen, C., Raulefs, R., and Aboutanios, E., "Recent Advances in Indoor Localization: A Survey on Theoretical Approaches and Applications," *IEEE*, 2009.

[15] Shen, G., Zetik, R., Yan, H., Hirsch, O., and Thoma, R. S., "Time of Arrival Estimation for Range-Based Localization in UWB Sensor Networks," *Proceedings of 2010 IEEE International Conference on Ultra-Wideband*, IEEE, Saint-Malo, France, 2010.

[16] Dashti, M., Ghoraishi, M., Haneda, K., and ichi Takada, J., *High-Precision Time-of-Arrival Estimation for UWB Localizers in Indoor Multipath Channels*, Novel Applications of the UWB Technologies, inTech, Shanghai, 2011, pp. 397–422.

[17] Alarifi, A., Al-Salman, A., Alsaleh, M., Alnafessah, A., Al-Hadhrami, S., Al-Ammar, M. A., and Al-Khalifa, H. S., "Ultra Wideband Indoor Positioning Technologies: Analysis and Recent Advances," *Sensors*, Vol. 16, No. 707, 2016, pp. 1–36.

[18] Hui Liu, P. B., Houshang Darabi, and Liu, J., "Survey of Wireless Indoor Positioning Techniques and Systems," *IEEE Journal*, Vol. 37, No. 6, 2007, pp. 1067–1080.

[19] Jarvis, R., Mason, A., Thornhill, K., and Zhang, B., "Indoor Positioning System," Louisiana State University, 2011, pp. 1–126.

[20] Decawave (ed.), *MDEK1001 Kit User Manual Module Development & Evaluation Kit for the DWM1001*, 2017.

[21] Decawave (ed.), *DWM1001 Firmware API Guide*, 2017.

[22] Decawave (ed.), *DWM1001 Datasheet*, 2017.

Name: Hannah Scheaffer

Major: Biochemistry

Faculty Mentor, Department: Dr. Matthew Ross, Dept. of Basic Sciences, College of Vet. Medicine

Title: Inactivation of Prostaglandin D_2 Glyceryl Ester Hydrolysis Using Carboxylesterase 1 Inhibitors Augments its Anti-inflammatory Effects in Human THP1 Monocytic/Macrophage Cells

Abstract

Human monocytic cells in blood have important roles in host defense and express the enzyme carboxylesterase 1 (CES1). This metabolic serine hydrolase plays a critical role in the metabolism of many molecules, including lipid mediators called prostaglandin glycerol esters (PG-Gs), which are formed during cyclooxygenase-mediated oxygenation of the endocannabinoid 2-arachidonoylglycerol. Some PG-Gs have been shown to exhibit anti-inflammatory effects. However, they are unstable compounds and their hydrolytic breakdown generates pro-inflammatory prostaglandins. We hypothesized that by blocking the ability of CES1 in monocytes/macrophages to hydrolyze PG-Gs, the beneficial effects of anti-inflammatory PGD2-G could be augmented. The goal of this study was to determine whether PGD2-G is catabolized by CES1, then to evaluate the degree to which this metabolism is blocked by small-molecule inhibitors. A human monocytic cell line (THP1 cells) was pretreated with increasing concentrations of small-molecule inhibitors that block CES1 activity [chlorpyrifos oxon (CPO), WWL229, or WWL113], followed by incubation with PGD2-G (10 μM). Organic solvent extracts of the treated cells were prepared and analyzed by LC-MS/MS to assess levels of the hydrolysis product PGD2. Further, THP1 monocytes with normal CES1 expression (control cells) and knocked down CES1 expression (CES1KD cells) were employed to confirm CES1's role in PGD2-G catabolism. We found that CES1 has a prominent role in PGD2-G hydrolysis in this cell line, accounting for about 50% of its hydrolytic metabolism, and that PGD2-G could be stabilized by the inclusion of CES1 inhibitors. The inhibitor potency followed the rank order: CPO>WWL113>WWL229. THP1 macrophages co-treated with WWL113 and PGD2 prior to stimulation with lipopolysaccharide exhibited a more pronounced attenuation of pro-inflammatory cytokine levels (IL-6) than by PGD2 treatment alone. These results suggest that the anti-inflammatory effects induced by PGD2-G can be further augmented by inactivating CES1 activity with specific small-molecule inhibitors.

Background

Carboxylesterase 1 (CES1) is a hydrolytic enzyme that plays a role in the hydrolysis of many types of compounds including prostaglandin glycerol esters. One of these, prostaglandin glycerol ester D2 (PGD2-G), has been shown to have anti-inflammatory effects in the white blood cells of the body. These effects are lost, however, in the hydrolyzed compound. We hypothesized that the PGD2-G compound could in fact be metabolized by the CES1 protein and that by inhibiting the enzyme, the amounts of the glycerol ester PGD2-G could be stabilized, increasing its anti-inflammatory effects. This is an important concept when considering possible ways to treat and cure inflammatory diseases like atherosclerosis and other autoimmune diseases.

Methods

Our specific objectives for this research project were to:

1. Add small-molecule inhibitor compounds to immune cells that express CES1, such as the THP1 cell line, to assess whether CES1 function in living cells can be inactivated.
2. Determine whether inactivating cellular CES1 function will decrease the production of PGD2 when cells are exposed to exogenously added PGD2-G.
3. Assess the potency of each small-molecule inhibitor with respect to their ability to block the hydrolytic degradation of PGD2-G to PGD2.
4. Investigate the effects of blocking the PGD2-G hydrolysis with an inhibitor on the levels of proinflammatory cytokine mRNA in LPS-treated macrophages.

We used a variety of methods to fulfill these objectives. First, we incubated intact THP1 monocytes, with increasing concentrations of our inhibitors (CPO, WWL113, or WWL229) and PGD2-G. The lipid soluble compounds were then extracted using ethyl acetate and the resulting solution was analyzed by lipid chromatography mass spectroscopy (LC-MS/MS). CES1 KD (knockdown) cells and Control cells were also incubated with PGD2-G and the resulting extracted solutions analyzed by LC-MS/MS as well. The purpose of these experiments was to determine if the PGD2-G was broken down by the CES1, if an inhibitor could stop the hydrolysis, and if so, by how much. These results were then compared to the results from the samples using CES1KD cells to see which process, gene knockdown or inhibition was more effective.

Control cell samples treated with WWL229 inhibitor were also prepared for testing in an Activity Based Protein Profiling (ABPP) gel. These samples were run through an ABPP gel and transferred to a membrane, then to film, so the results could be clearly seen and analyzed. The results showed the activity of the CES1 enzyme. This same membrane was stripped, and used to test for the presence of the CES1 protein in a Western Blot study. The results showed the amount CES1 in each sample. These tests were a confirmation that CES1 was the enzyme active in the hydrolysis of PGD2-G and that the inhibitor was effective in blocking its activity.

Finally, Control cells were differentiated into macrophages, and treated with WWL113 inhibitor, PGD2-G, and lipopolysaccharide (LPS). The LPS is an inflammatory agent. The idea was to block the CES1 by inhibitor, then add the anti-inflammatory compound, PGD2-G, and finally to inflame the cell with LPS and test the levels of inflammation by calculating the resulting mRNA levels for certain proinflammatory cytokines. The presence of the anti-inflammatory molecule should bring down the inflammation levels and the presence of the inhibitor increase the effect of the PGD2-G.

Results and Conclusions

We found that PGD2-G is catabolized by CES1 in monocytic cells and that CES1 is responsible for about 50% of its hydrolysis. We realized that by adding a small molecule inhibitor, either CPO, WWL113, or WWL229, the production of PGD2 decreased in the cells, dependent on the inhibitor concentration, indicating that the CES1 functions were blocked and the enzyme was less active in breaking down the original glycerol ester. The results from the CES1 Activity Based Protein Profiling gel and CES1 Western Blot support this result because they show that even though there is CES1 protein present in the cell samples, as the concentration of inhibitor increases, activity noticeably decreases. Overall, CPO was the most effective inhibitor and WWL229 the least effective, though WWL229 is more selective for CES1

than CPO. We also looked at the stabilization of PGD2-G amounts in cells that had knocked down CES1 expression, however, it seemed that using an inhibitor was actually more effective. As an inhibitor's concentration can be controlled, the levels of CES1 inhibition and therefore the amounts of anti-inflammatory PGD2-G can be controlled. It is through this controlled stabilization of cellular PGD2-G levels by blocking CES1 activity that the anti-inflammatory processes mediated by PGD2-G might be augmented. For example, mRNA levels of proinflammatory cytokine IL-6 were decreased in the presence of anti-inflammatory glycerol ester PGD2-G, and these effects were augmented by the CES1 inhibitor WWL113. Future research will continue to explore this relationship.

References

Alhouayek M., Buisseret B., Paquot A., Guillemot-Legris O., Muccioli GG. *The endogenous bioactive lipid prostaglandin D2-glycerol ester reduces murine colitis via DP1 and PPARγ receptors.* FASEB Journal. 2018 Sep; 32(9):5000-5011. doi: 10.1096/fj.201701205R. Epub 2018 Apr 9.

Alhouayek M., Masquelier J, Cani PD, Lambert DM, Muccioli GG. *Implication of the anti-inflammatory bioactive lipid prostaglandin D2-glycerol ester in the control of macrophage activation and inflammation by ABHD6*. Proc Natl Acad Sci U S A. 2013 Oct 22; 110(43):17558-63. doi:10.1073/pnas.1314017110. Epub 2013 Oct 7.

Alhouayek M., Masquelier J., Muccioli GG. *Controlling 2-arachidonoylglycerol metabolism as an anti-inflammatory strategy.* Drug Discov Today. 2014 Mar; 19(3):295-304. doi: 10.1016/j.drudis.2013.07.009.

Alhouayek M., Muccioli GG. *COX-2-derived endocannabinoid metabolites as novel inflammatory mediators.* Trends Pharmacol Sci. 2014 Jun; 35(6):284-92. doi:10.1016/j.tips.2014.03.001. Epub 2014 Mar 29. Epub 2013 Jul 23.

Name: Ciarra Smith
Major: Biochemistry
Faculty Mentor, Department: John Bickle, Ph.D., Department of Philosophy and Religion

Title: Effects of Explanatory Sciences on Moral Responsibility

Introduction

Advances in neuroscience explore how the microscopic cells in our brains influence our day to day activities. In order to raise a hand, the brain interprets a complex medley of chemical messengers that indicate which muscles should flex and relax at precisely the right time. As neuroscientists gain ground in our scientific understanding of the relationship between neuronal signaling and behaviors, there appears to exist a direct correlation between brain states and behaviors. This directional relationship presents an interesting twist for individuals forced to make evaluative judgments on the actions of others. If our actions are simply an expression of chemical reactions in the brain, and we cannot directly control those reactions, are we truly responsible for our actions?

Background

Non-experts of the sciences are often asked to make evaluative judgments on the actions of others in the presence of scientific information. The aim of this study is to evaluate how the inclusion of explanations from various sciences influence the judgments of moral responsibility and evaluate which field, if any, holds more influential power. The research will address the interaction between sciences with high behavioral explanatory power and moral decision making by measuring the perception of responsibility post-exposure to scientific information in comparison to a no explanation control group.

> H1: Evidence from social-psychology and experimental philosophy studies indicate participants are more likely to reduce attribution of moral responsibility in the negative scenario comparatively to the positive or neutral scenario (Rahimi, Hall, & Pychyl, 2016).
> H2: Scientific explanations based on physiology (genetic and neuroscience) will have greater influence in reducing participants' judgments on moral responsibility.
> RQ1: Among competing theories for human behavior (genetics, neuroscience, environmental influence) which theory, if any, holds more prominent authority over beliefs about moral responsibility?
> RQ2: What are the moderating effects of participant characteristics (e.g., Belief in Free Will) on the likelihood of altered judgments in moral responsibility?

Method

The study will utilize a 3 (scenario: positive, neutral, or negative) X 4 (explanation for behavior: genetic, neuroscience, environmental influence, no explanation control) between-subjects experimental design. This experiment embedded in a web-based survey will be administered to

roughly 300 Amazon Mechanical workers (MTurk) aged 18 and older and living in the U.S. The survey is divided into two parts.

Part 1 contains the experimental manipulation. Participants will view one of 3 vignettes describing an actor committing either a moral or immoral action based on work by Knutson et al, 2010. Participants will then be provided with one of 3 possible explanations for the actor's behavior that includes either genetic, neuroscientific, or environmental factors. Participants in the control group will not be presented with a possible scientific explanation. All participants will be asked to evaluate the moral responsibility, blameworthiness, and recidivism of the actor as well as assess the morality of the action. After the evaluation, participants will be given a short recall test asking the participant to recall the action committed and the type of explanation (genetic, neuroscientific, or environmental) provided for that action. In Part 2, participants will be asked questions about possible moderating variables, including deference to scientific authority, belief in free will, and science-literacy.

Expected Results & Discussion

This study is ongoing. Expected results should follow previous research in that a higher reduction of moral responsibility will be attributed to actors conducting morally wrong actions with provided physiological explanations (genetics and neuroscience) (Aspinwall, Brown, & Tabery, 2012). It is likely that individuals with a lesser science-literacy score will ascribe the greatest reduction in moral responsibility to the experimental actor. Science-literacy refers to an individual's (National Academy Press, 1998). A low science-literacy score is not a direct indication of a person's level of education but reflects the individual's comfort in questioning natural phenomenon and evaluating evidence.

In addition to variations in science-literacy as a possible contributor to reducing responsibility, neuroscience information, in particular, has been known to interfere with people's judgments. In one study on the influence of neuroscience information specifically, the researchers found the mere presence of neuroscience language caused non-experts to look more favorably on material they would have ordinarily found to be faulty (Weisberg, Keil, Goodstein, Rawson, & Gray, 2008). It is possible that when presented with neuroscience information, the participants fall victim to a reasoning heuristic in which technical language is naturally seen as more favorable (Weisberg et al., 2008). While our study cannot yet conclude why neuroscience information is apparently mesmerizing to the point of distraction, once completed, we can provide some indication as to the relative seductive nature of neuroscience information comparatively to other sciences that similarly provide technical explanations for phenomena.

References

Aspinwall, L. G., Brown, T. R., & Tabery, J. (2012). The Double-Edged Sword: Does Biomechanism Increase or Decrease Judges' Sentencing of Psychopaths? *Science*, *337*(6096), 846–849. https://doi.org/10.1126/science.1219569

Knutson, K. M., Krueger, F., Koenigs, M., Hawley, A., Escobedo, J. R., Vasudeva, V., …

Grafman, J. (2010). Behavioral norms for condensed moral vignettes. *Social Cognitive and Affective Neuroscience*, 5(4), 378–384. https://doi.org/10.1093/scan/nsq005

National Academy Press. (1998). Principles and Definitions. *National Science Education Standards* (pp. 19 – 26). Washington, DC: National Academy of Sciences.

Rahimi, S., Hall, N. C., & Pychyl, T. A. (2016). Attributions of Responsibility and Blame for Procrastination Behavior. *Frontiers in Psychology*, 7. https://doi.org/10.3389/fpsyg.2016.01179

Weisberg, D. S., Keil, F. C., Goodstein, J., Rawson, E., & Gray, J. R. (2008). The Seductive Allure of Neuroscience Explanations. *Journal of Cognitive Neuroscience*, *20*(3), 470–477. https://doi.org/10.1162/jocn.2008.20040

Name: AlliGrace Story

Major: Psychology

Faculty Mentor, Department: Dr. Cliff McKinney, Psychology

Title: *Effects of Parental Internalizing Problems on Irritability in Adolescents: Moderation by Parental Warmth and Overprotection*

Research has consistently demonstrated a link between parental and offspring psychopathology (Dougherty et al., 2013; Eyre et al., 2017; Low et al., 2012; Walker & McKinney, 2015). Previous research also has shown that parenting factors including warmth (opposite being rejection; Goldner et al., 2016) and overprotection (opposite being autonomy granting; Borelli, Margolin, & Rasmussen, 2015) affect the relationship between parent and child psychopathology. However, relatively less research has examined how these parenting factors affect the relationship between parental internalizing problems and child irritability specifically, which is especially relevant given that the prevalence of irritability has increased over time (Collishaw, Maughan, Natarajan, & Pickles, 2010). Past research also has shown that parent and child gender affect offspring outcomes (Antúnez, De la Osa, Granero, and Ezpeleta, 2016; Kashdan et al., 2004; Trepat, Granero, & Ezpeleta, 2014; Wiggins, Mitchell, Stringaris, & Leibenluft, 2014). Thus, the current study examined the moderating role of parental warmth and overprotection in the relationship between parental internalizing problems and adolescent irritability from the perspective of parents.

Parent-Offspring Psychopathology

Previous research has shown a link between parental and offspring broad psychopathology in emerging adults (Walker & McKinney, 2015). More specifically, research has linked maternal internalizing problems with offspring internalizing problems in emerging adults (Low et al., 2012), parental depression and anxiety with offspring irritability in children aged 3 to 6 years (Dougherty et al., 2013), and child depression and anxiety with child irritability in children 6 to 18 years (Eyre et al., 2017). Additionally, mothers of children aged 1 to 9 years with more severe irritability, relative to those with less, were more likely to have recurrent depression (Wiggins et al., 2014). Whelan, Leibenluft, Stringaris, and Barker (2015) found that maternal depressive symptoms prenatally and postnatally were related to toddler temperament factors, which predicted child irritability, which in turn predicted depressive symptoms during adolescence. Similarly, Antúnez and colleagues (2016) found that child temperament traits were associated with higher levels of oppositional defiant disorder (ODD) symptoms, including irritability and defiance, and that paternal anxiety and depression strengthened this relationship.

Gender also affects the relationship between parental and offspring psychopathology. For example, although both maternal and paternal alcohol abuse predicted severity of child irritability, only maternal drug abuse predicted severity of child irritability (Wiggins et al, 2014). Additionally, paternal, but not maternal, anxiety and depression moderated the relationship between child temperament traits and child ODD (Antúnez et al., 2016). Research also has demonstrated that relationship quality between mothers and emerging adult sons was related to internalizing and externalizing problems in sons and that maternal externalizing problems were indirectly associated with internalizing and externalizing problems in sons through relationship quality (Franz & McKinney, 2018).

Parental Warmth and Overprotection

Studies have shown that parenting factors such as warmth and overprotection affect the relationship between parent and offspring psychopathology. For example, high maternal warmth predicted higher resilience in young adults (Pargas, Brennan, Hammen, & Le Brocque, 2010). However, paternal, but not maternal, depression was associated with lower parental warmth (Epkins & Harper, 2016). Additionally, maternal depression was associated with less positive reactions with children (Hummel, Kiel, & Zvirblyte, 2015) and maternal anxiety was associated with higher maternal overprotection and lower maternal warmth (Drake & Ginsburg, 2011). Therefore, parental psychopathology plays an important role in parents maintaining warm relationships with their children. In contrast, parental overprotection has been linked with anxiety symptoms in children that persisted over time, and maternal overprotection played a mediating role between maternal and child anxiety (Borelli et al., 2015). Additionally, parents with anxiety tended to be more perfectionistic and, therefore, more overprotective when parenting, which was associated with child anxiety (Affrunti & Woodruff-Borden, 2015).

Parental factors also can affect child irritability. For example, parents who had more positive parenting beliefs perceived their children as less irritable (Chen & Luster, 1999), and, more specifically, children of warmer parents were less irritable (Prinzie et al., 2004). Other research has found that maternal corporal punishment mediated the relationship between maternal psychopathology and ODD symptoms including irritability (Trepat et al., 2014), and maternal involvement acted as a moderator that protected against the development of ODD symptoms (Li, Clark, Klump, & Burt, 2017). Additionally, parental anxiety was associated with increased parental intrusiveness and negative discipline, increased parental social distress, and decreased parental warmth and positive involvement, which in turn were related to child ODD symptoms including irritability (Kashdan et al., 2004).

In addition to affecting the link between parental and offspring psychopathology, gender also affects parenting behaviors. For example, Kashdan et al. (2004) found that mothers tended to use less warmth and positive involvement and more intrusiveness and negative discipline than fathers. Additionally, Trepat et al. (2014) found that maternal corporal punishment mediated the relationship between maternal anxiety and depression and child ODD symptoms for preschool girls, whereas it mediated maternal aggressive behavior and child ODD symptoms for boys. Paternal parenting behaviors did not mediate paternal psychopathology and child ODD symptoms; however, paternal psychopathology did have a direct effect on child ODD symptoms (Trepat et al., 2014). In a study using emerging adults, males perceived less authoritative parenting, more permissive parenting, and more parental psychological aggression and physical assault than emerging adult females and perceived mothers to be more authoritarian than fathers (McKinney, Brown, & Malkin, 2017).

Several studies have shown that maternal warmth and overprotection often were related to child outcomes, whereas paternal warmth and overprotection were more frequently not. For example, high maternal warmth predicted higher resilience in young adults (Pargas et al., 2010), whereas low maternal warmth predicted child anxiety (Drake & Ginsburg, 2011). Additionally, maternal overprotection played a mediating role in the relationship between maternal anxiety and child anxiety (Borelli et al., 2015). Furthermore, although paternal, but not maternal, depression was related to lower parental warmth (Epkins & Harper, 2016), maternal anxiety was associated with high maternal overprotection and low maternal warmth (Drake & Ginsburg, 2011).

Current Study

Although the prevalence of irritability has been shown to increase over time (Collishaw et al., 2010), less research has examined how parenting factors, such as parental internalizing

problems and warmth and overprotection, affect offspring irritability, particularly in the context of gender. Also, recent research has begun to consider adolescence as encompassing a larger time period than the traditional time frame associated with adolescence due to changes in societal norms (Sawyer, Azzopardi, Wickremarathne, & Patton, 2018). For example, people tend to pursue education for a longer period of time, get married at older ages, and have children at older ages, which results in an extended transition into adulthood; additionally, the onset of adolescence has been extended to an earlier age due to early puberty (Sawyer et al., 2018). Thus, the current study examined how parental warmth and overprotection moderated the relationship between parental internalizing problems and offspring irritability in a sample of parents of adolescents aged 10 to 24 years.

Hypothesis 1 stated that parental internalizing problems would be positively related with adolescent irritability and parental overprotection and negatively related with parental warmth. Hypothesis 2 stated that parental warmth would be negatively related and parental overprotection would be positively related with adolescent irritability. Hypothesis 3 stated that the relationship between parental internalizing problems and child irritability would be stronger in the context of higher parental overprotection and weaker in the context of higher parental warmth (i.e., moderation by parental warmth and overprotection). Hypothesis 4 stated that maternal warmth and overprotection would have a stronger moderating effect than paternal warmth and overprotection (i.e., moderation by parent gender).

Method

Participants

Participants included parents of adolescents aged 10 to 24 years, given that Sawyer et al. (2018) defined adolescence as the ages of 10 to 24 years. As shown in Table 1, the highest

percentage of parent participants as well as the child's other primary caregiver reported on by participants were aged 35 to 44 years, were Caucasian, had received a bachelor's degree, and were employed. Children of the parent participants were primarily male and Caucasian and had not yet received a high school degree. The number of children at each age tends to decrease as age increases.

Measures

Parental internalizing problems and adolescent irritability. The Adult Self-Report (ASR; Achenbach & Rescorla, 2003) and the Adult Behavior Checklist (ABCL; Achenbach & Rescorla, 2003) were used to measure internalizing problems of the parent and the adolescent's other primary caregiver, as well as adolescent irritability based on the perceptions of the parent taking the survey. The ASR and ABCL include 123 items that measure internalizing and externalizing problems. Internalizing problems were measured using the Anxious/Depressed (e.g., *worries about his/her future*; *feels worthless or inferior*), Withdrawn (e.g., *refuses to talk*), and Somatic Problems Syndrome (e.g., *headaches*) subscales. Responses ranged from *not true* to *very true or often true.* The ASR and ABCL have demonstrated good psychometrics overall and are valid tools when used to report on others' behaviors as long as raters are familiar with the ratee (e.g., parents rating their children or children's other caregiver; Rescorla & Achenbach, 2004). Adolescent irritability also was measured using an irritability dimension derived from an ODD problem scale created through confirmatory factor analysis. This scale included 5 problems reflecting irritability (e.g., *hot temper, irritable, get upset too easily*). Although some participants reported on children outside the normative range of the ASR/ABCL (i.e., younger than 18 years), the irritability items from the ASR/ABCL were considered developmentally appropriate for this age range and have corresponding items on parallel forms for younger age groups (e.g., the Child

Behavior Checklist). Thus, the use of a single measure was deemed appropriate to avoid instrumentation, especially given that similar items are assessed across the parallel forms.

Parental warmth and overprotection. The Parental Bonding Instrument (PBI; Parker, Tupling, & Brown, 1979) measured maternal and paternal warmth and overprotection from the perspective of the parent taking the survey. The measure includes two variables, which are warmth (e.g., *speak to my child with a warm and friendly voice*), with the opposite extreme being indifference or rejection (e.g., *seem emotionally cold to my child*), and overprotection (e.g., *am overprotective of my child*), with the opposite extreme being encouragement of autonomy (e.g., *let my child decide things for himself or herself*). The measure includes 25 items, with responses ranging from *very like* to *very unlike* on a 4-point Likert scale. The PBI demonstrated good to excellent internal consistency, as it has had split-half reliability coefficients of .88 for care and .74 for overprotection in other studies. The PBI also demonstrated good stability, as it has had three-week test-retest reliabilities of .76 for care and .63 for overprotection, and good concurrent validity, as it correlates significantly with independent rater judgments of parental caring and overprotection.

Procedure

Participants read a brief description of the study on the Amazon Mechanical Turk website and were able to click a link to the survey. Before beginning the survey, participants completed qualification questions to ensure that they had an adolescent child within the age range of 10 to 24 years. Participants who qualified were then provided an informed consent form electronically before beginning the survey. Participants first completed a demographic form about themselves and were instructed to report on their oldest child in the 10 to 24 year range. Afterwards, they completed the ASR/ABCL and PBI about themselves in random order. This process was

repeated for the child's other primary caregiver. Lastly, participants completed a demographic form about their child and then completed the ASR/ABCL about their child. After completing the survey, participants were provided a debriefing form electronically.

Planned Analyses

Hypotheses 1 and 2 were tested by conducting path analysis as shown in Figure 1 using AMOS 24.0. Hypothesis 3 was tested by building interaction terms between parental internalizing problems and parental warmth and overprotection; significant interactions were standardized and plotted at +/- 1 *SD* for interpretation. Hypothesis 4 was tested by using pairwise parameter comparisons, which produces a *Z* score indicating differences between paths, similar to comparing correlation coefficients; specifically, maternal and paternal interaction effects were compared.

Results

As shown in Table 2, results indicated that the parent participants' internalizing problems were correlated positively with the other primary caregiver's internalizing problems, child irritability, and their own and the other caregiver's overprotection, and correlated negatively with their own warmth and the other caregiver's warmth. Adolescents' other primary caregivers' internalizing problems also were correlated positively with adolescent irritability, the parent participants' overprotection, and their own overprotection, and correlated negatively with the parent participants' warmth and their own warmth. The parent participants' warmth was correlated positively with the other caregivers' warmth, and correlated negatively with their own overprotection and the other caregivers' overprotection. Adolescent irritability was correlated positively with both the parent participants' and the other caregivers' overprotection, and was correlated negatively with both the parent participants' and the other caregivers' warmth.

To test hypotheses, path analysis was used as displayed in Figure 1. Direct effects from the path analysis are displayed in Table 3. Supporting hypothesis 1 (i.e., parental internalizing problems would be negatively related with adolescent irritability and parental overprotection and negatively related with parental warmth), parental internalizing shared a positive association with adolescent irritability and parental overprotection and a negative association with parental warmth. In support of hypothesis 2 (i.e., parental warmth would be negatively related and parental overprotection would be positively related with adolescent irritability), parental warmth had a negative association with adolescent irritability, whereas parental overprotection shared a positive association with adolescent irritability. In partial support of hypothesis 3 (i.e., the relationship between parental internalizing problems and adolescent irritability would be stronger in the context of higher parental overprotection and weaker in the context of higher parental warmth), the interaction between parental warmth and internalizing problems on adolescent irritability was significant. See Figure 2 for a plot of this interaction. Parents who reported high internalizing problems and low warmth also reported more irritability in their adolescents relative to the other groups, whereas parents who reported high warmth and low internalizing problems also reported the lowest irritability in their adolescents. However, parent and child gender were not significant moderators of this interaction.

Parental overprotection demonstrated several significant interactions including the 4-way interaction of parental overprotection x parental internalizing problems x parent gender x child gender. See Figure 3 for the plot of this 4-way interaction, which also displays all lower order interactions. Female adolescents were reported as having higher irritability when mothers reported higher internalizing problems relative to lower internalizing problems, regardless of maternal overprotection, with these effects being within 0.5 *SD* of the mean. Male adolescents

whose mothers reported high overprotection and high internalizing problems were reported to have the most irritability of all the groups, whereas male adolescents whose mothers reported low overprotection and high internalizing problems were reported as having the lowest irritability of all the groups. For the paternal figure, male adolescents were reported as having more irritability than females when fathers reported themselves as low in overprotection and high in internalizing problems. However, female adolescents were reported as having more irritability than males when fathers reported themselves as high in overprotection and high in internalizing problems. When paternal overprotection and internalizing problems were both low, male adolescents were reported as having higher irritability than females; these male adolescents also reported less irritability than male adolescents whose fathers reported themselves as high in both overprotection and internalizing problems. Furthermore, when paternal overprotection was high and paternal internalizing problems was low, female adolescents were reported as having more irritability than male adolescents but less irritability than females whose fathers reported both low overprotection and internalizing problems.

Discussion

The current study examined how parental warmth and parental overprotection moderated the relationship between parental internalizing problems and irritability in adolescents aged 10 to 24 years. Past research consistently uses children as participants, especially when the child is over 18 years of age (Inguglia et al., 2016; Stevens, Bardeen, & Murdock, 2015); however, the parents were the participants in the current study, providing a unique perspective. Additionally, the current study examined the effects of parental internalizing, parental warmth and overprotection, and adolescent irritability in the context of parent and child gender. Results indicated that parental warmth and overprotection significantly moderated the relationship

between parental internalizing problems and adolescent irritability, although parent and child gender did not affect this relationship when examining warmth but did affect this relationship when examining overprotection.

Results supporting Hypothesis 1 were consistent with past research that showed associations between parental internalizing problems and offspring irritability (Dougherty et al., 2013), better outcomes with higher maternal warmth (Pargas et al., 2010), and associations between parental internalizing problems and parental warmth (Epkins & Harper, 2016).Parental internalizing problems and offspring irritability often are associated because offspring could learn irritable behaviors from observing their parents who have internalizing problems (i.e., modeling) (Ginicola, 2007). Additionally, offspring who have parents who are irritable may be treated more harshly by their parents and respond with irritable behaviors, as well as any conferred genetic risks (Roberson-Nay et al., 2015).

Results supporting Hypothesis 2 also were consistent with past research demonstrating that parental warmth was negatively associated with adolescent irritability, whereas parental overprotection was associated positively (Prinzie et al., 2004). A possible explanation for the negative association between parental warmth and adolescent irritability is that parental warmth improves the parent-child relationship (Nelson, Padilla-Walker, Christensen, Evans, & Carroll, 2011), which might influence adolescents' perceptions of the parent-child relationship to be more positive, thus decreasing their irritability. In contrast, adolescents may perceive parental overprotection as negative and overly controlling, so they may become more irritable in response.

Results supporting Hypothesis 3 showed that parental warmth moderated the relationship between parental internalizing problems and adolescent irritability. These results are consistent

with past research showing that parental warmth acts as a protective factor against the development of internalizing problems (Goldner et al., 2016). However, parent and child gender did not moderate this relationship, which may mean that boys and girls interpret maternal and paternal warmth in a similar way. Another possible explanation for this finding is that mothers and fathers may not differ in how they exhibit warmth to their sons and daughters when considering internalizing problems as opposed to more overt stressors such as perceived neighborhood danger as studied by Goldner and colleagues (2016).

In partial support of Hypothesis 4, parental overprotection also moderated the relationship between parental internalizing and adolescent irritability, and parent and child gender further moderated this relationship. Results indicated that maternal overprotection was more strongly associated with irritability in male adolescents than female adolescents, indicating a strong effect for mother-son dyads. The effect for mother-son dyads could be stronger because of the way male adolescents interpret maternal overprotection, as compared to how they interpret paternal overprotection. For example, male adolescents may see maternal overprotection as mothers' being antagonistic, which has been shown to be negatively associated with male adolescents' ability to self-regulate (Moilanen, Shaw, & Fitzpatrick, 2010), which could lead to high irritability.

Similarly, male adolescents were reported to have more irritability when their mothers had high overprotection, whereas they were reported to have less irritability when their fathers had high overprotection. It could be the case that male adolescents interpret parental overprotection differently when it comes from their mother instead of their father. For example, perceived paternal modeling of masculine norms and perceived paternal sexist communication indirectly mediated the relationship between perceived paternal authoritarianism and sons'

sexism (Klann, Wong, & Rydell, 2018). It is possible that sons view overprotection as the father's responsibility according to the traditional view of the father being the head of the household. Thus, males may interpret their father's overprotection as a positive form of caring, and a lack of overprotection from fathers as the father not caring, which could lead to high irritability.

Implications

Future research should examine the potential applications of the findings from the current study. For example, since the results indicated gender differences in regard to parental overprotection, future research should further examine these effects. Future research should also further examine gender effects on parenting and psychopathology and how the effects develop longitudinally. The gender effects that were found in the current study also indicate that clinicians should take parent and child gender into account when planning how to approach therapy, especially family therapy that may address problems related to irritability, parental overprotection, and internalizing problems. Such clinical considerations would be best informed by more rigorous research as suggested here.

Limitations and Strengths

The current study exhibited some limitations. For example, the study relied on the reports of the parent participants in examining psychopathology and behaviors of the parent participant, the adolescent's other primary caregiver, and the adolescent. Since the parent participant reported on the adolescent and the other caregiver, the reports of psychopathology and parenting behaviors might not be as accurate as for the child and other caregiver as they are for the parent participant. Additionally, the current study relied on cross-sectional data, so no causal conclusions can be drawn. Furthermore, participants were primarily Caucasian, which leads to an

underrepresentation of other races, so results may not generalize to populations with more racial diversity. However, groups are better represented in other demographic areas, such as age and gender.

The current study also demonstrated several strengths. For example, the current study found significant gender differences in the relationship between parental internalizing, parental overprotection, and adolescent irritability, which identifies particular gender dyads that may be problematic in adolescents' development of irritability problems.

References

Achenbach T. M.,& Rescorla L. A. (2003). *Manual for the ASEBA adult forms & profiles*. University of Vermont, Research Center for Children, Youth, & Families, Burlington, VT.

Affrunti, N. W., & Woodruff-Borden, J. (2015). Parental perfectionism and overcontrol: Examining mechanisms in the development of child anxiety. *Journal of Abnormal Child Psychology, 43,* 517-529. doi:10.1007/s10802-014-9914-5

Antúnez, Z., de la Osa, N., Granero, R., & Ezpeleta, L. (2016). Parental psychopathology levels as a moderator of temperament and Oppositional Defiant Disorder symptoms in preschoolers. *Journal of Child and Family Studies*, *25*, 3124-3135. doi:10.1007/s10826-016-0461-2

Borelli, J. L., Margolin, G., & Rasmussen, H. F. (2015). Parental overcontrol as a mechanism explaining the longitudinal association between parent and child anxiety. *Journal of Child and Family Studies, 24,* 1559-1574. doi:10.1007/s10826-014-9960-1

Collishaw, S., Maughan, B., Natarajan, L., & Pickles, A. (2010). Trends in adolescent emotional problems in England: A comparison of two national cohorts twenty years apart. *Journal of Child Psychology and Psychiatry, 51,* 885-894. doi:10.1111/j.1469-7610.2010.02252.x

Chen, F., & Luster, T. (1999). Factors related to parenting behavior in a sample of adolescent mothers with two-year-old children. *Early Child Development and Care, 153*, 103-119. doi:10.1080/0300443991530106

Dougherty, L. R., Smith, V. C., Bufferd, S. J., Stringaris, A., Leibenluft, E., Carlson, G. A., & Klein, D. N. (2013). Preschool irritability: Longitudinal associations with psychiatric disorders at age 6 and parental psychopathology. *Journal of the American Academy of*

Child & Adolescent Psychiatry, 52, 1304-1313. doi:10.1016/j.jaac.2013.09.007

Drake, K. L., & Ginsburg, G. S. (2011). Parenting practices of anxious and nonanxious mothers: A multi-method, multi-informant approach. *Child & Family Behavior Therapy, 33,* 299-321. doi:10.1080/07317107.2011.623101

Epkins, C. C., & Harper, S. L. (2016). Mothers' and fathers' parental warmth, hostility/rejection/neglect, and behavioral control: Specific and unique relations with parents' depression versus anxiety symptoms. *Parenting: Science and Practice, 16,* 125-142. doi:10.1080/15295192.2016.1134991

Eyre, O., Langley, K., Stringaris, A., Leibenluft, E. Collinshaw, S., & Thapar, A. (2017). Irritability in ADHD: Associations with depression liability. *Journal of Affective Disorders, 215,* 281-287. doi:10.1016/j.jad.2017.03.50

Franz, A. O., McKinney, C. (2018). Parental and child psychopathology: Moderated mediation by gender and parent-child relationship quality. *Child Psychiatry & Human Development,* doi:10.1007/s10578-018-0801-0

Ginicola, M. M. (2007). Children's unique experience of depression: Using a developmental approach to predict variation in symptomatology. *Child and Adolescent Psychiatry and Mental Health*, *1*. https://doi.org/10.1186/1753-2000-1-9

Goldner, J. S., Quimby, D., Richards, M. H., Zakaryan, A., Miller, S., Dickson, D., & Chilson, J. (2016). Relations of parenting to adolescent externalizing and internalizing distress moderated by perception of neighborhood danger. *Journal of Clinical Child and Adolescent Psychology, 45,* 141-154. doi:10.1080/15374416.2014.958838

Hummel, A. C., Kiel, E. J., & Zvirblyte, S. (2016). Bidirectional effects of positive affect, warmth, and interactions between mothers with and without symptoms of depression and

their toddlers. *Journal of Child and Family Studies, 25,* 781-789. doi:10.1007/s10826-015-0272-x

Inguglia, C., Ingoglia, S., Liga, F., Lo Coco, A., Lo Cricchio, M. G., Musso, P., & … Lim, H. J. (2016). Parenting dimensions and internalizing difficulties in Italian and U.S. emerging adults: The intervening role of autonomy and relatedness. *Journal of Child and Family Studies, 25*, 419-431. doi:10.1007/s10826-015-0228-1

Kashdan, T. B., Jacob, R. G., Pelham, W. E., Lang, A. R., Hoza, B., Blumenthal, J. D., & Gnagy, E. M. (2004). Depression and Anxiety in Parents of Children With ADHD and Varying Levels of Oppositional Defiant Behaviors: Modeling Relationships With Family Functioning. *Journal Of Clinical Child And Adolescent Psychology*, *33*(1), 169-181. doi:10.1207/S15374424JCCP3301_16

Klann, E. M., Wong, Y. J., & Rydell, R. J. (2018). Firm father figures: A moderated mediation model of perceived authoritarianism and the intergenerational transmission of gender messages from fathers to sons. *Journal of Counseling Psychology, 65*, 500–511. https://doi.org/10.1037/cou0000296

Li, I., Clark, D. A., Klump, K. L., & Burt, S. A. (2017). Parental involvement as an etiological moderator of middle childhood oppositional defiant disorder. *Journal Of Family Psychology*, *31*, 659-667. doi:10.1037/fam0000311

Low, N. C., Dugas, E., Constantin, E., Karp, I., Rodriguez, D., & O'Loughlin, J. (2012). The association between parental history of diagnosed mood/anxiety disorders and psychiatric symptoms and disorders in young adult offspring. *BMC Psychiatry, 12,* 188. doi:10.1186/1471-244X-12-188

McKinney, C., Brown, K., & Malkin, M. L. (2017). Parenting style, discipline, and parental

psychopathology: Gender dyadic interactions in emerging adults. *Journal of Child and Family Studies,* doi:10.1007/s10826-017-0865-7

Moilanen, K. L., Shaw, D. S., & Fitzpatrick, A. (2010). Self-regulation in early adolescence: Relations with mother–son relationship quality and maternal regulatory support and antagonism. *Journal of Youth and Adolescence, 39*, 1357–1367. https://doi.org/10.1007/s10964-009-9485-x

Nelson, L. J., Padilla-Walker, L. M., Christensen, K. J., Evans, C. A., & Carroll, J. S. (2011). Parenting in emerging adulthood: An examination of parenting clusters and correlates. *Journal of Youth and Adolescence*, *40*, 730–743. https://doi.org/10.1007/s10964-010-9584-8

Pargas, R. C. M., Brennan, P. A., Hammen, C., & Le Brocque, R. (2010). Resilience to maternal depression in young adulthood. *Developmental Psychology, 46*, 805-814. doi:10.1037/a0019817

Parker, G., Tupling, H., & Brown, L. (1979). A parental bonding instrument. *British Journal of Medical Psychology*, *52*, 1-10.

Prinzie, P., Swillen, A., Maes, B., Onghena, P., Vogels, A., Van Hooste, A., & ... Fryns, J. (2004). Parenting, family contexts, and personality characteristics in youngsters with VCFS. *Genetic Counseling: Medical, Psychological, and Ethical Aspects, 15*, 141-157.

Rescorla, L., & Achenbach, T. (2004). The Achenbach System of Empirically Based Assessment (ASEBA) for ages 18 to 90 years. The use of psychological testing for treatment planning and outcomes assessment. In *Instruments for adults* (3rd ed., Vol. 3). Mahwah, NJ US: Lawrence Erlbaum Associates Publishers.

Roberson-Nay, R., Leibenluft, E., Brotman, M. A., Myers, J., Larsson, H., Lichtenstein, P., &

Kendler, K. S. (2015). Longitudinal stability of genetic and environmental influences on irritability: From childhood to young adulthood. *The American Journal of Psychiatry, 172*, 657–664. https://doi.org/10.1176/appi.ajp.2015.14040509

Sawyer, S. M., Azzopardi, P. S., Wickremarathne, D., & Patton, G. C. (2018). The age of adolescence. *The Lancet Child and Adolescent Health, 2,* 223-228.

Stevens, E. N., Bardeen, J. R., & Murdock, K. W. (2015). Parenting behaviors and anxiety in young adults: Effortful control as a protective factor. *Journal of Individual* Differences, 36, 170-176. doi: 10.1027/1614-0001/a000169

Trepat, E., Granero, R., & Ezpeleta, L. (2014). Parenting practices as mediating variables between parents' psychopathology and oppositional defiant disorder in preschoolers. *Psicothema*, *26*(4), 497-504.

Walker, C. S., & McKinney, C. (2015). Parental and emerging adult psychopathology: Moderated mediation by gender and affect toward parents. *Journal of Adolescence, 44*, 158-167. doi: 10.1016/j.adolescence.2015.07.016

Whelan, Y. M., Leibenluft, E., Stringaris, A., & Barker, E. D. (2015). Pathways from maternal depressive symptoms to adolescent depressive symptoms: The unique contribution of irritability symptoms. *Journal of Child Psychology and Psychiatry, 56,* 1092-1100. doi:10.1111/jcpp.12395

Wiggins, J. L., Mitchell, C., Stringaris, A., & Leibenluft, E. (2014). Developmental trajectories of irritability and bidirectional associations with maternal depression. *Journal of the American Academy of Child & Adolescent Psychiatry, 53,* 1191-1205. doi:10.1016/j.jaac.2014.08.005

Table 1

Demographic Information

	Parent Participant	Other Caregiver	Child
Age	38.5% 35-44 years 32.8% 25-34 years 21.7% 45-54 years 4.0% 55-64 years 2.6 % other	28.5% 35-44 years 22.7% 45-54 years 17.7% 25-34 years 6.8% 18-24 years 6.5% 17 years or younger 5.8% 55-64 years 2.0% other	26.3% 10-12 years 21.6% 13-15 years 17.9% 16-18 years 9.3% 19-21 years 6.8% 22-24 years
Gender	58.9 % Female 41.1% Male	59.2% Male 31.2% Female	59.4% Male 30.2% Female
Race	74.6% Caucasian 16.3% African American 9.1% Other	68.2% Caucasian 14.1% African American 8.1% Other	64.0% Caucasian 15.3% African American 10.4% Other
Education	39.8% bachelor's degree 18.9% master's degree 16.6% Some college but no degree 9.7% Other 6.5% High school graduate	29.2% bachelor's degree 14.6% Some college but no degree 14.3% master's degree 13.4% High school graduate 9.5% Other	49.9% Less than high school degree 14.3% High school graduate 8.4% Other 8.8% bachelor's degree 8.1% Some college but no degree
Employment	88.6% Working 10.3% Not working	76.3% Working 12.6% Not working	31.4% Working 56.3% Not working

Table 2

Descriptive Statistics and Correlations

	1.	2.	3.	4.	5.	6.	7.	M	SD	Max	α
1. Parent Internalizing	1							23.08	19.03	75.00	.97
2. Other Internalizing	.84*	1						20.15	19.78	78.00	.98
3. Adolescent Irritability	.69*	.70*	1					2.56	2.76	10.00	.86
4. Parent Warmth	-.65*	-.62*	-.58*	1				27.62	6.87	36.00	.88
5. Parent Overprotection	.51*	.49*	.41*	-.54*	1			14.28	6.16	32.00	.76
6. Other Warmth	-.42*	-.47*	-.36*	.49*	.26*	1		24.27	8.47	36.00	.91
7. Other Overprotection	.41*	.46*	.35*	-.47*	.56*	-.36*	1	14.28	6.96	33.00	.80

Note. * indicates $p < .01$. All minimum = 0.

Table 3

Path Coefficients

	Child Irritability
Warmth	-.22*
Overprotection	.19*
Internalizing	.40*
Child Gender	-.03
Child Age	.05
Parent Gender	.04
Parent Age	-.03
Parent Race	-.04
Parent Education	.04
Parent Relationship Status	-.05
Parent Gender x Child Gender	.03
Warmth x Internalizing	-.08*
Warmth x Parent Gender	.02
Warmth x Child Gender	.01
Warmth x Internalizing x Child Gender	-.02
Warmth x Internalizing x Parent Gender	-.05
Warmth x Internalizing x Parent Gender x Child Gender	.04
Overprotection x Internalizing	.21*
Overprotection x Parent Gender	.13*
Overprotection x Child Gender	-.32*
Overprotection x Internalizing x Child Gender	-.07*
Overprotection x Internalizing x Parent Gender	.05
Overprotection x Internalizing x Parent Gender x Child Gender	-.16*

Note. * indicates $p < .01$.

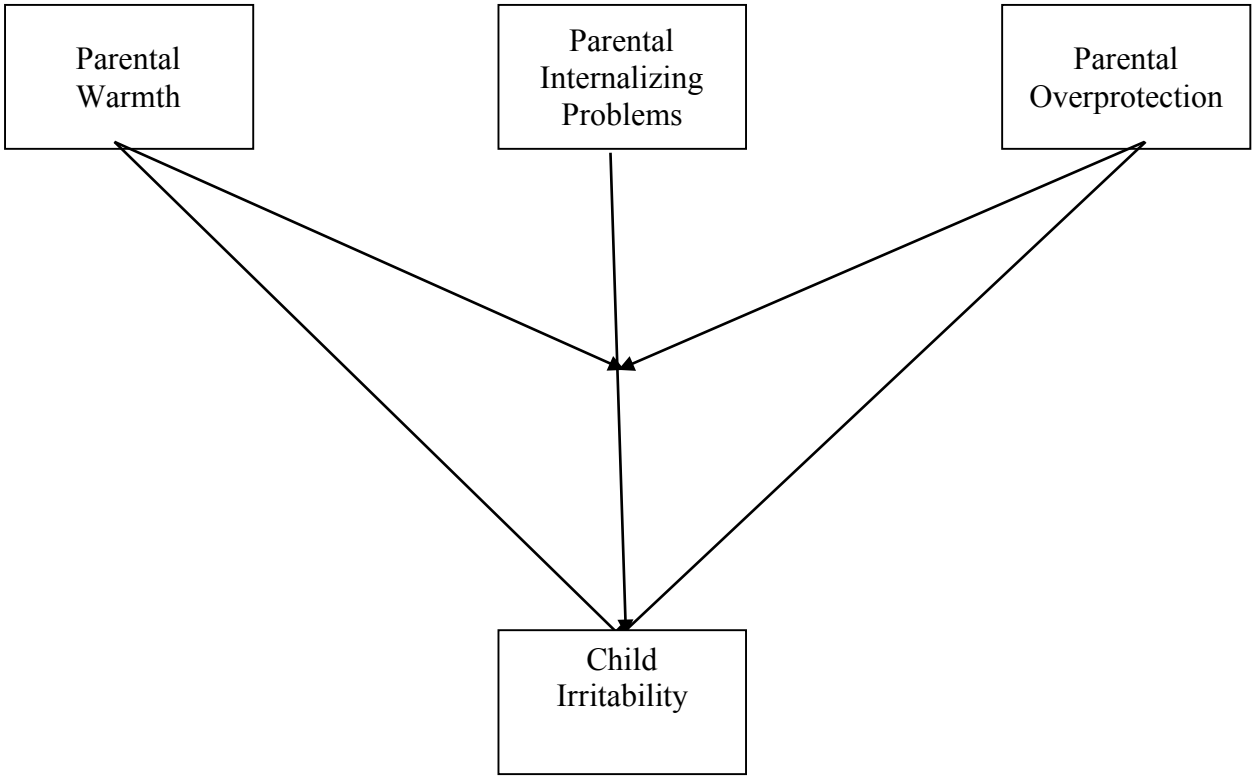

Figure 1. Conceptual model of path analysis.

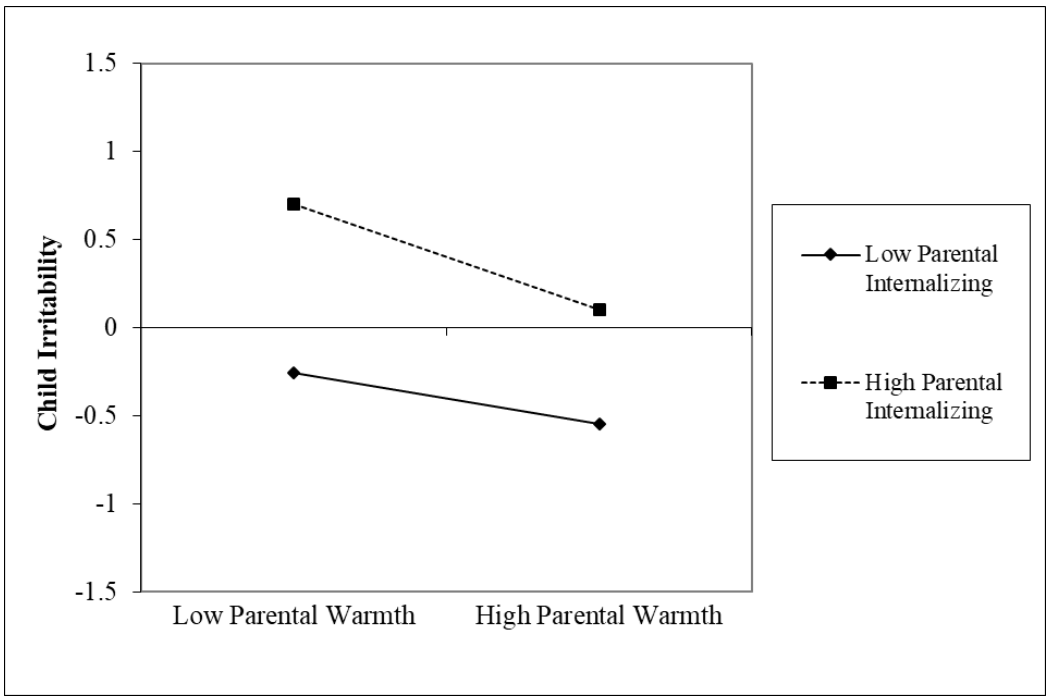

Figure 2. Parental Warmth x Parental Internalizing interaction on Child Irritability. Parent and child gender were not significant moderators.

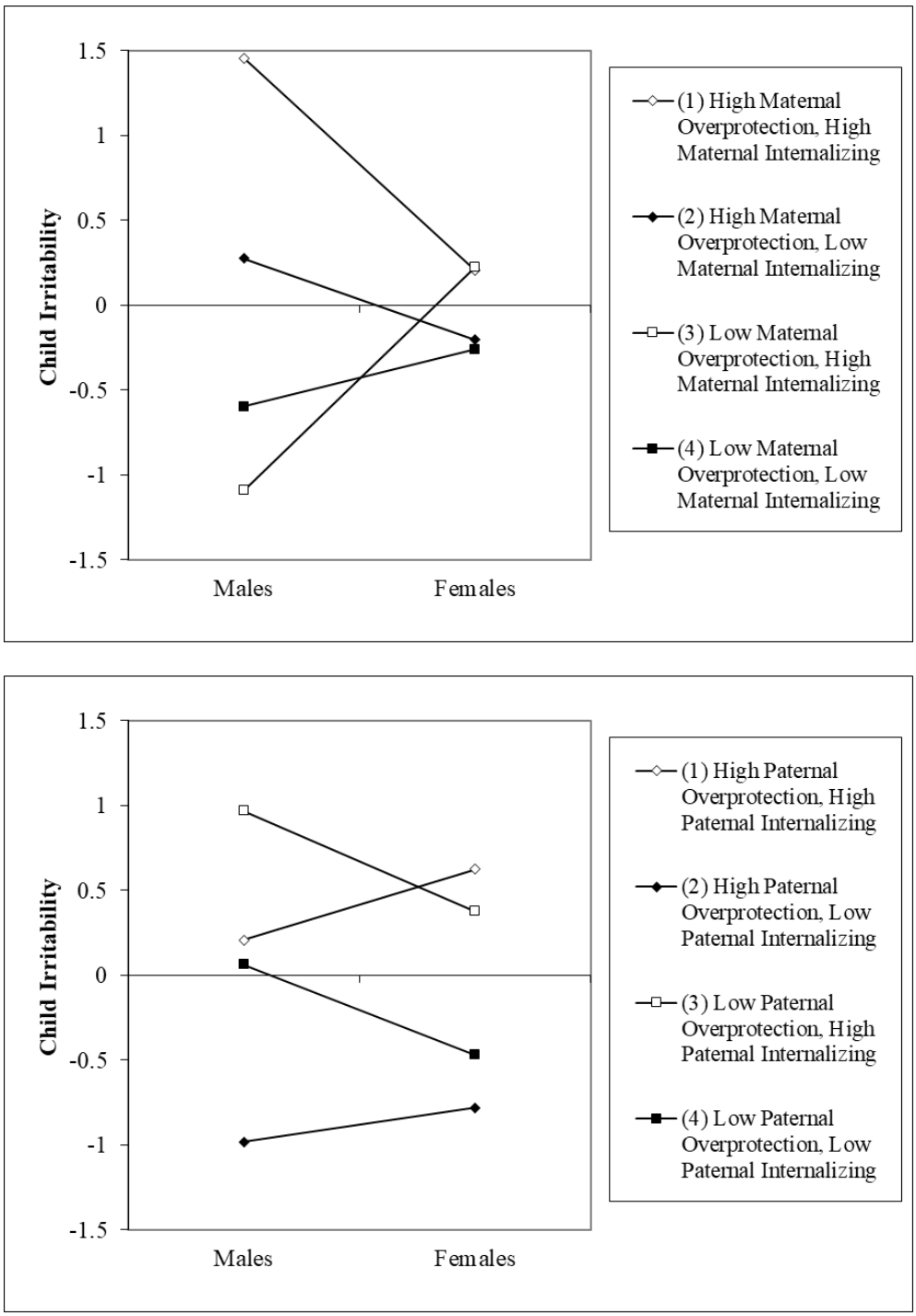

Figure 3. Parental Overprotection x Parental Internalizing x Parent Gender x Child Gender interaction on Child Irritability. Top figure represents maternal variables and bottom figure represents paternal variables.

Assessment of Diversity of a captive population of Seba's short-tailed bats (*Carollia perspicillata*)

Undergraduate Researcher: Allison Watwood, BCH-EPP
Faculty Supervisor, Department: Federico G. Hoffmann, BCH-EPP, Biochemistry, Molecular Biology, Entmology & Plant Pathology

A. Purpose

Seba's short-tailed bat is a small, fruit-eating Neotropical bat of the family Phyllostomidae with a wide geographic distribution that ranges from Southern Brazil to Mexico. They also serve as a research model in studies of animal energetics, flight aerodynamics, physiology, reproduction and animal behavior. Because of their unusually long life for an animal of its size and the fact that its colonies can be maintained with success, this species is garnering attention as a model to understand mammalian senescence (Fasel, Saladin, Richner 2016). In fact, *Carollia perspicillata* is the most bred bat species in captivity. Unfortunately, most captive colonies were established without a clear understanding of the genetic diversity present in the wild and several colonies are beginning to show signs of inbreeding. Thus, there is a need to develop breeding practices that take genetic diversity into account and to better understand what might be leading to some reproductive problems in these colonies. The goal of the current project is the first step in this direction. Our objective is to assess the genetic diversity of the captive bat population located at the Papiliorama, a tropical zoo, in Kerzers FR, Switzerland using sequences from the mitochondrial cytochrome-b gene. This population was originally founded with specimens from Brazil and Costa Rica, which represent different genetic lineages of this species, but its current genetic composition is unclear. Previous research carried out by FG Hoffmann identified four separate genetic lineages, with some overlap in their geographic distributions. Specimens from Costa Rica would be expected to come from the northern lineage, whereas the specimens from Brazil could represent any of the other genetic lineages in this species. Determining this is of key importance to develop a management plan. A priori, there are two reasonable and competing explanations that could account for the observed difficulties in breeding: 1) lack of genetic diversity in the captive population or 2) breeding between individuals from lineages that are not fully compatible at the genetic level, as some of these lineages might represent incipient species. Assessing the current diversity of the captive population is a necessary first step to discern between these alternatives.

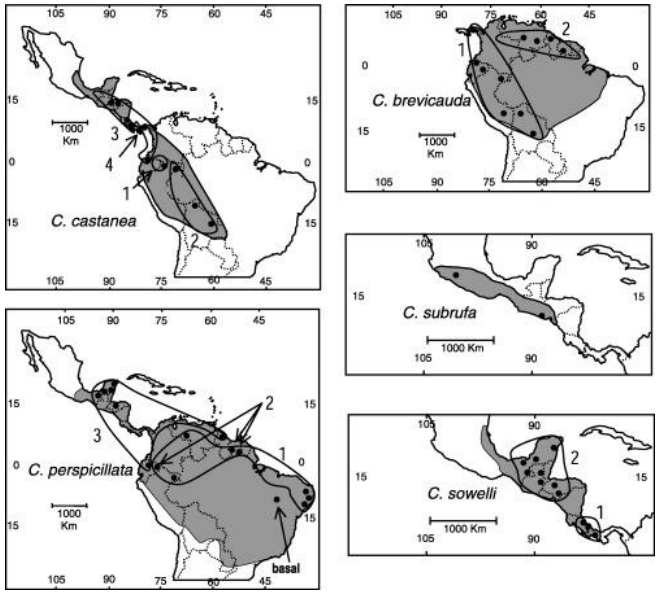

Figure 1: Geographic distribution of short-tailed bats of the genus Carollia, modified from Pine (1972), with phylogroups within each species identified by closed lines. Numbers correspond to the phylogroups defined in the text. In the case of C. perspicillata, sampling localities for the basal branch and phylogroup 2 are identified by arrows. (Hoffmann, Baker 2003)

B. Significance of the project

The current project is a collaboration between Federico Hoffmann, from BCH-EPP at MSSTATE, and Dr. Nicolas Fasel, from the Leibniz Institute for Zoo and Wildlife Research, who is in charge of the Papiliorama. Dr. Nicolas Fasel has extensive experience using this bat colony for research in reproductive physiology and is interested in developing a sustainable management plan for this colony as well as in understanding what might be driving differences in reproductive success. Dr. Federico Hoffmann is an Associate Professor in the Department of Biochemistry, Molecular Biology, Entomology and Plant Pathology at Mississippi State that worked on understanding the geographic distribution of genetic variation in bats of the genus *Carollia* for his doctoral dissertation. At present, he is interested in the evolution of animal genomes and in the role small RNAs might play in divergence among closely related lineages. Recent research in *Drosophila* suggests small RNAs and their protein counterparts might play a more central role in reproductive incompatibilities than previously anticipated. Dr. Hoffmann and Dr. Fasel are likely to pursue this research further, if this was the case. Personally, this project would allow me to gain experience in collecting and analyzing data by integrating my background in bioinformatics and wet lab techniques in order to answer two very concrete questions: How diverse is the bat population of the Papiliorama tropical zoo? and Which genetic lineages are currently represented in the population?

C. Materials and Methods

The current project has three components. The first involves wet lab work at Mississippi State: extracting DNA from skin punches of bats using the DNEasy DNA extraction kit and amplification of a portion of the mitochondrial cytochrome-b gene using primers and conditions described in Hoffmann and Baker (2003). The second phase will be Sanger-sequencing of the PCR products using Global Biologics. Then the last part will be analyzing the the resulting data in our lab using MEGA, MUSCLE, and IQTree. Basically, the resulting sequences will be aligned to the data set used for the original 2003 manuscript to place them in a phylogenetic context and also estimate basic measures of diversity for the captive colony.

D. Results

DNA was successfully extracted from all 42 tissue samples using the DNEasy extraction kit. Each sample produced two 50µL vials of eluted DNA. The DNA was then ran through gel electrophoresis to check for DNA product, which all came back positive. The eluted DNA was amplified using a polymerase chain reaction (PCR) protocol. Through gradient testing, it was determined the optimum temperature for the PCR protocol was 54°C. After the first round of PCR, a double band was illuminated in the diagnostic gel. This means the primers were hitting in more than one place in the genome. We specifically wanted the cytochrome-b portion of the mitochondrial genome to be amplified, but we believe the primers could be hitting a paralog in the nuclear genome. I even tried to extract the desired DNA through gel extraction, but this did not produce quality results. We are currently in the process of designing new primers to more specifically amplify the correct portion of the *Carollia perspicillata* mitochondrial genome. After the amplification, the PCR product will be Sanger sequenced and analyzed; this process should not take longer than two weeks.

E. IRB and IACUC Approval

IRB and IACUC approval is not needed for the research being performed. Skin punches have been collected following approved protocols from Papiliorama.

F. References

Fasel, Nicolas & Saladin, Verena & Richner, Heinz. (2016). Alternative reproductive tactics and reproductive success in male Carollia perspicillata (Seba's short-tailed bat). Journal of evolutionary biology. 29. 10.1111/jeb.12949.

Hoffmann, Federico & J Baker, R. (2004). Comparative phylogeography of short-tailed bats (Carollia: Phyllostomidae). Molecular ecology. 12. 3403-14. 10.1046/j.1365-294X.2003.02009.x.